Industrial Waste Water Treatment through Vacuum Membrane Distillation

A Final Year Project Report

Presented to

SCHOOL OF MECHANICAL & MANUFACTURING ENGINEERING

Department of Mechanical Engineering

NUST

ISLAMABAD, PAKISTAN

In Partial Fulfillment
of the Requirements for the Degree of
Bachelors of Mechanical Engineering

by

Muhammad Shaheryar Baig
Muhammad Sohail Umer
Saqib Ali
Hafiz Umer Afzal

May 2019

EXAMINATION COMMITTEE

We hereby recommend that the final year project report prepared under our supervision by:

Muhammad Shaheryar Baig	00000132751
Muhammad Sohail Umer	00000125491
Saqib Ali	00000122718
Hafiz Umer Afzal	00000138363

Titled: "Industrial waste water treatment through Vacuum Membrane Distillation" be accepted in partial fulfillment of the requirements for the award of BE MECHANICAL degree

Supervisor: Muhammad Sajid, Dr.	Dated:
Committee Member: Emad ud Din, Dr.	Dated:
Committee Member: Zaib Ali, Dr.	Dated:

_____ _____

(Head of Department) (Date)

COUNTERSIGNED

Dated: _____ _____

(Dean / Principal

ABSTRACT

Vacuum membrane distillation technique is employed to purify industrial waste water. This technique is a very handy solution to the current water challenges. The feed water enters the test section from one side and evaporates. The vapors than pass through a hydrophobic membrane to the permeate side. The driving force is vacuum pressure generated by vacuum pump on the permeate side. Mathematical modelling is conducted to know the effects of temperature, feed velocity and pressure difference. The temperature is increased through a heat exchanger.

ACKNOWLEDGMENTS

The authors are thankful to the faculty supervisor, AP Dr. Muhammad Sajid, whose continuous guidance and encouragement over the entire course of the project helped us overcome obstacles faced during the various stages of the project. We believe his high expectations and regular involvement in the project are the reasons for the quality of the work that has been produced till this day.

ORIGINALITY REPORT

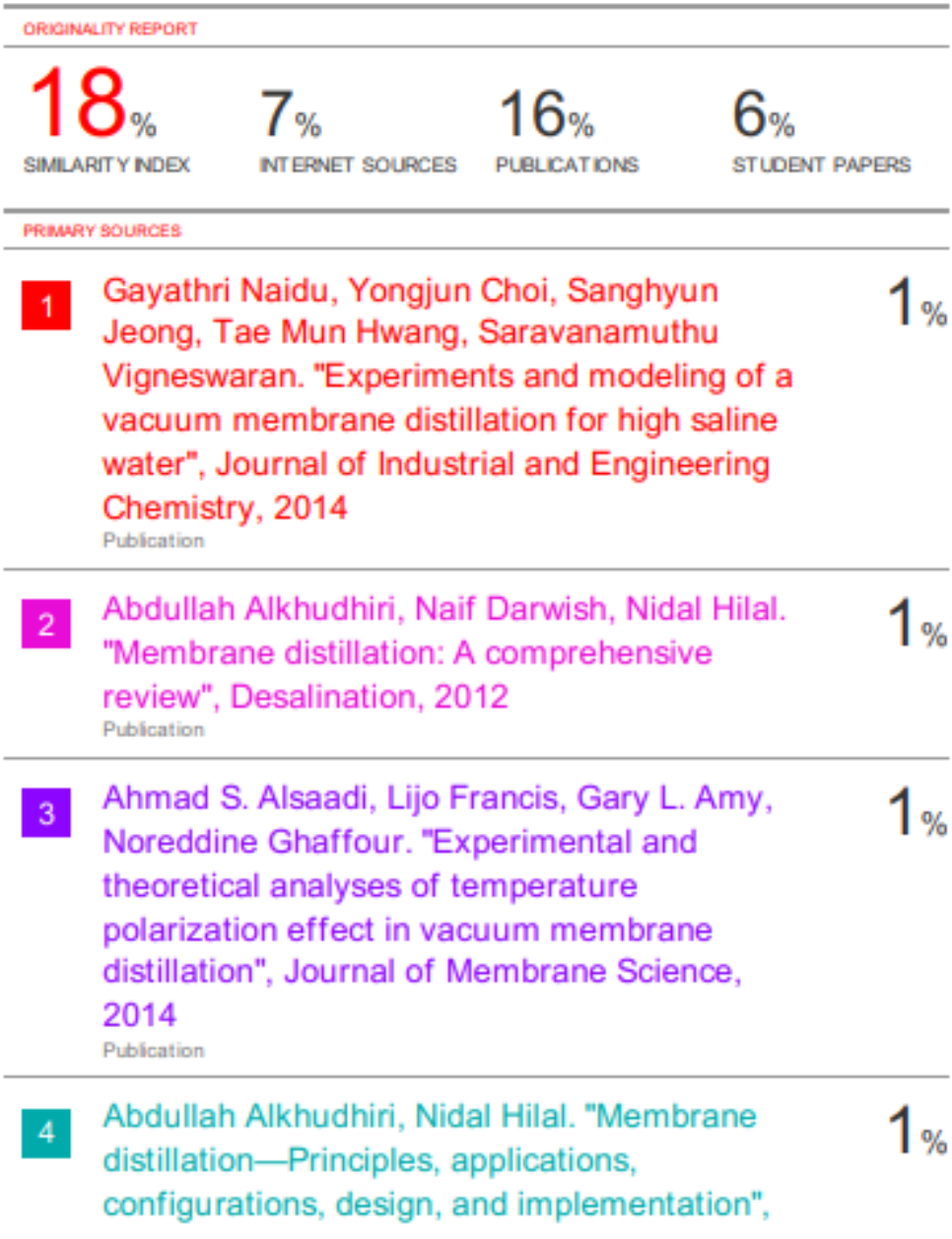

ORIGINALITY REPORT

18%	7%	16%	6%
SIMILARITY INDEX	INTERNET SOURCES	PUBLICATIONS	STUDENT PAPERS

PRIMARY SOURCES

1	Gayathri Naidu, Yongjun Choi, Sanghyun Jeong, Tae Mun Hwang, Saravanamuthu Vigneswaran. "Experiments and modeling of a vacuum membrane distillation for high saline water", Journal of Industrial and Engineering Chemistry, 2014 Publication	1%
2	Abdullah Alkhudhiri, Naif Darwish, Nidal Hilal. "Membrane distillation: A comprehensive review", Desalination, 2012 Publication	1%
3	Ahmad S. Alsaadi, Lijo Francis, Gary L. Amy, Noreddine Ghaffour. "Experimental and theoretical analyses of temperature polarization effect in vacuum membrane distillation", Journal of Membrane Science, 2014 Publication	1%
4	Abdullah Alkhudhiri, Nidal Hilal. "Membrane distillation—Principles, applications, configurations, design, and implementation",	1%

	Elsevier BV, 2018 Publication	
5	Parimal Pal. "Arsenic Removal by Membrane Distillation", Elsevier BV, 2015 Publication	1%
6	aaltodoc.aalto.fi Internet Source	1%
7	Submitted to Caledonian College of Engineering Student Paper	1%
8	J.I. Mengual, M. Khayet, M.P. Godino. "Heat and mass transfer in vacuum membrane distillation", International Journal of Heat and Mass Transfer, 2004 Publication	1%
9	qspace.qu.edu.qa Internet Source	1%
10	Fan, Hongwei, and Yuelian Peng. "Application of PVDF membranes in desalination and comparison of the VMD and DCMD processes", Chemical Engineering Science, 2012. Publication	1%
11	Mostafa Abd El-Rady Abu-Zeid, Yaqin Zhang, Hang Dong, Lin Zhang, Huan-Lin Chen, Lian Hou. "A comprehensive review of vacuum membrane distillation technique", Desalination,	<1%

	2015 Publication	
12	Submitted to National University of Singapore Student Paper	<1%
13	Seunghwan Kim, Sewoon Kim, Zubair Ahmed, Daniel K. Cha, Jinwoo Cho. "Flux model for the membrane distillation process to treat wastewater: effect of solids concentration", Journal of Membrane Science, 2018 Publication	<1%
14	es.scribd.com Internet Source	<1%
15	rshanthini.com Internet Source	<1%
16	Chel-Ken Chiam, Rosalam Sarbatly. "Vacuum membrane distillation processes for aqueous solution treatment—A review", Chemical Engineering and Processing: Process Intensification, 2013 Publication	<1%
17	Biplob Kumar Pramanik, Kandasamy Thangavadivel, Li Shu, Veeriah Jegatheesan. "A critical review of membrane crystallization for the purification of water and recovery of minerals", Reviews in Environmental Science and Bio/Technology, 2016 Publication	<1%

18	M. Essalhi, M. Khayet. "Self-sustained webs of polyvinylidene fluoride electrospun nanofibers at different electrospinning times: 2. Theoretical analysis, polarization effects and thermal efficiency", Journal of Membrane Science, 2013 Publication	<1%
19	Submitted to University of Surrey Roehampton Student Paper	<1%
20	Mohamed Khayet. "Membrane Distillation", Advanced Membrane Technology and Applications, 09/12/2008 Publication	<1%
21	Submitted to International Islamic University Malaysia Student Paper	<1%
22	Lagana, F.. "Direct contact membrane distillation: modelling and concentration experiments", Journal of Membrane Science, 20000214 Publication	<1%
23	link.springer.com Internet Source	<1%
24	www.springer.com Internet Source	<1%

25	Submitted to University of Newcastle upon Tyne Student Paper	<1%
26	Alsaadi, Ahmad S., Lijo Francis, Gary L. Amy, and Noreddine Ghaffour. "Experimental and theoretical analyses of temperature polarization effect in vacuum membrane distillation", Journal of Membrane Science, 2014. Publication	<1%
27	pmworldlibrary.net Internet Source	<1%
28	www.ijser.org Internet Source	<1%
29	Dhananjay Singh, Lin Li, Gordana Obuscovic, John Chau, Kamalesh K. Sirkar. "Novel Cylindrical Cross-Flow Hollow Fiber Membrane Module for Direct Contact Membrane Distillation-based Desalination", Journal of Membrane Science, 2017 Publication	<1%
30	El-Bourawi, M.S.. "A framework for better understanding membrane distillation separation process", Journal of Membrane Science, 20061115 Publication	<1%

SUPERVISOR: DR. MUHAMMAD SAJID. _____

DATED: _____

TABLE OF CONTENTS

CONTENTS

LIST OF TABLES

LIST OF FIGURES

ABBREVIATIONS

MD	Membrane Distillation
DCMD	Direct Contact Membrane Distillation
AGMD	Air Gap Membrane Distillation
SGMD	Sweeping Gas Membrane Distillation
VMD	Vacuum Membrane Distillation Volatile Organic
VOCs	Compounds Polytetrafluoroethylene Gained
PTFE	Output Ratio
GOR	Temperature Polarization Coefficient
TPC	

NOMENCLATURE

Kn	Knudsen number
Sc	Schmidt number
Re	Reynolds number
Nu	Nusselt number
T	Temperature (K)
P	Pressure (Pa)
x	Concentration (mol/dm^3)
J	Water vapor mass flux (kg/m^2*hr)
B_m	Net MD coefficient
r	Pore size (m)
ω	Percentage porosity of membrane
δ	Membrane thickness (m)
τ	Pore tortuosity
M	Molecular mass (kg/kmol)
R	General gas constant (J/mol.K)
Q	Heat transfer rate (W)
h	Convective coefficient of heat transfer
H_v	Latent heat of vaporization of water (J/kg)
K_m	Thermal conductivity of water
d_h	Hydraulic diameter (m)
k_B	Boltzmann constant
Φ	Sphericity of the particle making the medium
η	Viscosity
D	Diameter of particle making the medium
e	Porosity of the medium
R_v	Viscous Resistance
R_i	Inertial Resistance
u_m	mass-averaged velocity (m/s)
ρ_m	mixture density (kg/m^3)
α_k	volume fraction of phase k
N	number of phases
κ	turbulence kinetic energy (J)
ε	dissipation rate of κ(m^2/s)
F	body force(N)
μ_m	viscosity of the mixture (m/s)
C	

$u_{dr;k}$	Constant
k_{eff}	drift velocity for secondary phase k (m/s)
k_t	effective conductivity (W/(m·K)) turbulent thermal conductivity [W/(m·K)]

CHAPTER 1: INTRODUCTION

Motivation:

The Need for Clean Water

Water is an essential natural resource. It fuels the socio-economic development of nations. Agriculture, energy, industry, and the survival of life on Earth depend on the access to clean water. According to the United Nations, 2.1 billion people lack access to safely managed water services. Around 80% of all wastewater flows back into the ecosystem without being treated or reused [1].

Due to rapid population growth and increased burden on current water resources like rivers and lakes due to pollution and climate change, there is an immediate need to address the issue of water pollution and introduction of alternate methods of obtaining usable water for the people.

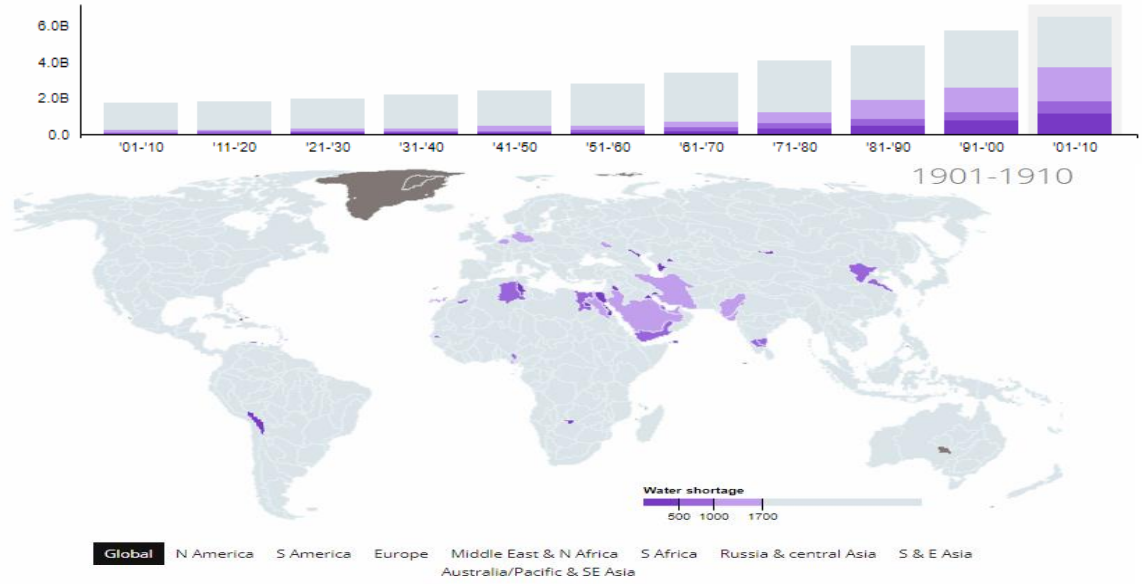

Figure 1- Water shortage index (Source: The United Nations World Water Development Report 2016)

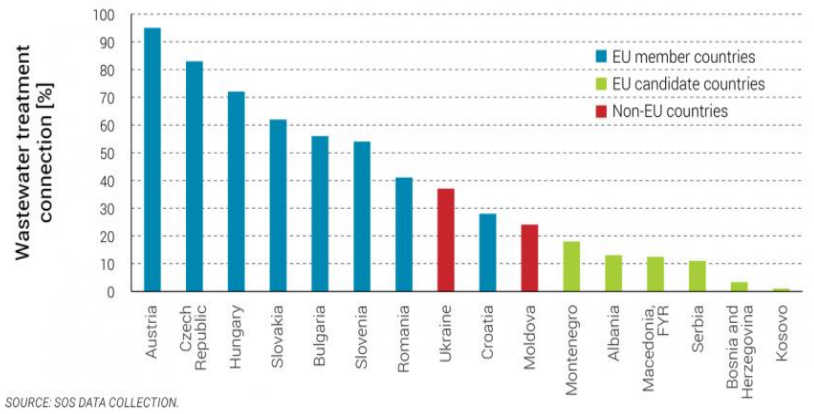

Figure 2- Statistics on wastewater treatment in different countries

Effect of industrial pollutants on environment and health

Inorganic salts containing metal and non-metal ions increase the water hardness levels and make them undesirable for application in industrial and agricultural setting. These salts can settle in water pipelines, thereby decreasing capacity. The dyeing process is affected by hardness of water. Highly mineralized water has a negative effect on marine life and human health. Industry effluents from leather tanneries have been observed to reduce plant growth. The deposition of salts decreases heat transfer in boilers and kettles. Chlorides are toxic to freshwater fish in excess of 400 ppm. Hexavalent chromium compounds are toxic if their concentration is greater than 5ppm. [2]

The fact that most of the industrial wastewater is discharged into water bodies without proper treatment produces an alarming danger to life of all types. To encourage adoption of treatment technologies, energy efficient and cost effective processes need to be introduced and made commercially available.

Working of Vacuum Membrane Distillation:

Membrane distillation is a promising answer to the water shortage problem. MD employs a hydrophobic membrane to separate salts from water due to pressure difference created between two chambers. Lower operating temperatures and hydrostatic pressure encountered in MD process make it a potential cost-effective substitute for conventional processes like Reverse Osmosis.

The MD process has a high rejection percentage for desalination of saline water. It has been employed to remove organic and heavy metals from aqueous solution. The MD system can be combined with other technologies like RO and ultrafiltration to improve process efficiency. MD has the ability to make use of renewable energy sources like solar energy and geothermal energy. [3-8]. As of writing this report, there is no study that investigates the removal of harmful salts from discharge of leather tanneries. For these reasons, the current project aims to fill this gap in the body of knowledge. It is hoped that the successful execution of this project will further the progress made by MD as a promising alternative to water treatment.

Problem Statement:

To investigate experimentally and theoretically the removal of metallic ions from industrial wastewater to produce drinkable water using Vacuum Membrane Distillation.

Objectives of the Project:

- To perform mathematical modelling of VMD process
- To undertake experimental study of VMD process
- Design and development of module

Project Plan:

The project plan is shown by the Gantt chart:

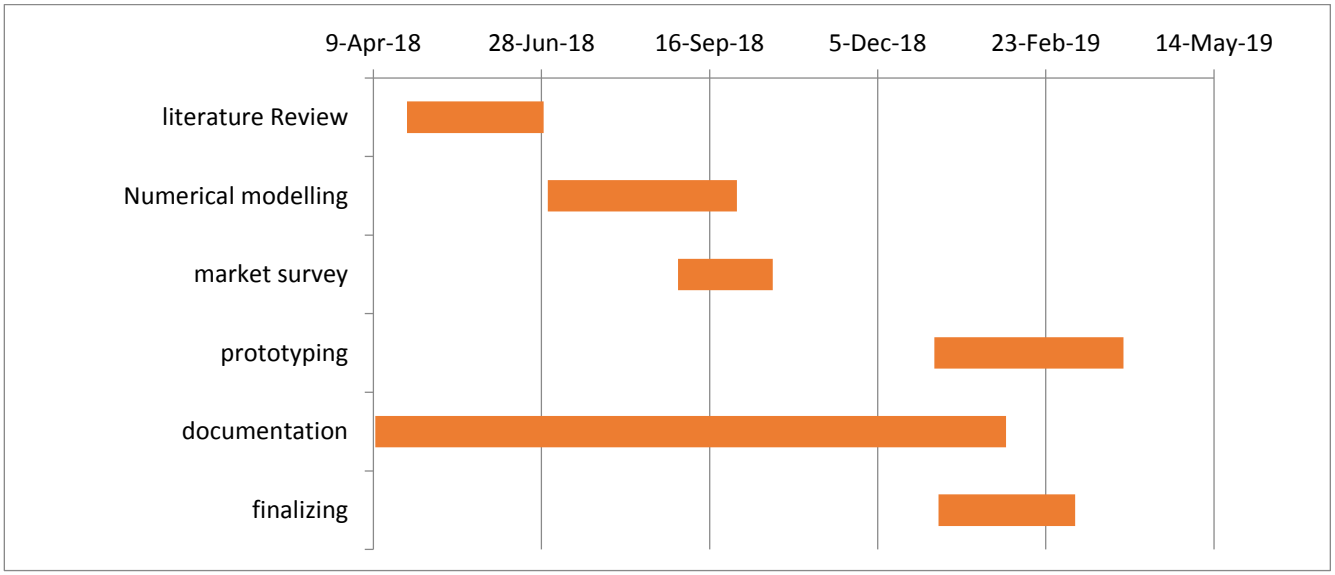

Figure 3- Gantt chart

CHAPTER 2: LITERATURE REVIEW

Membrane Distillation

Membrane Distillation is described as a thermally driven separation process in which water vapors are removed from an aqueous solution at a temperature less than 100*C using a hydrophobic membrane which separates two compartments, one which contains the feed solution while the other contains cold water, gas or vacuum [9,10] .

Types of Membrane Distillation

MD has four types:

Direct Contact Membrane Distillation

In a DCMD configuration (figure 5), there is a hot feed aqueous solution on entrance of the membrane and a cold permeate solution on the exit side. The pressure difference causes the water vapors to move across the membrane and then it condense in the permeate side. The water repellent characteristic of the membrane stops the liquid feed solution from entering the membrane while allowing the vapors to cross the membrane. DCMD is the simplest configuration employed widely for desalination and food processing applications. Due to the contact of water with the membrane on the permeate side, a lot of useful thermal energy is lost through conduction across the membrane. [11]

Air Gap Membrane Distillation

The heat lost hrough conduction in DCMD is reduced by introducing stagnant air between the membrane and the permeate condensation surface in AGMD (figure 7). The vapor crosses this air gap and condenses in the permeate side. The introduction of the air gap, however, introduces additional mass transfer resistance. This configuration is suitable for removal of VOCs from aqueous solution and desalination applications

Sweeping Gas Membrane Distillation

In SGMD (figure 4), a current of inert gas is used to remove vapors from the membrane on the permeate side which are condensed in an external condenser. This technique has a disadvantage that it uses a large volume of gas to sweep a very small amount of water vapors, thereby requiring a large condenser. Unlike DCMD, little energy is lost through conduction while at the same time the presence of moving gas instead of a stationary air gap as in AGMD reduced the mass transfer resistance. This technique is useful for removing VOCs from aqueous solutions. [12,16,17]

Vacuum Membrane Distillation

Both mass transfer resistance and energy loss are reduced in VMD (figure 6) by using a vacuum on the permeate side. The presence of vacuum creates a large pressure difference which enhances mass flux across membrane significantly. VMD has been used for several applications including brine treatment, removal of VOCs, wastewater treatment, and concentration of different solution

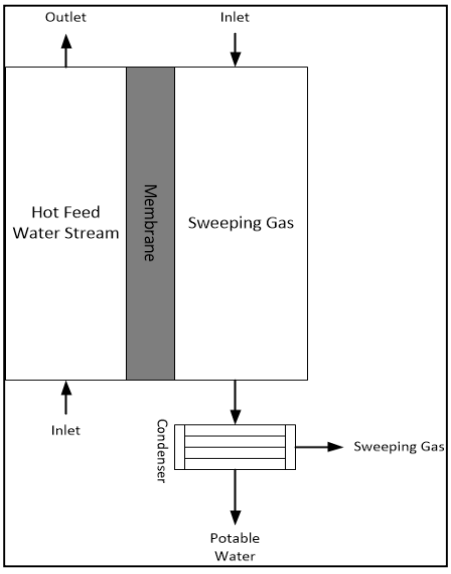

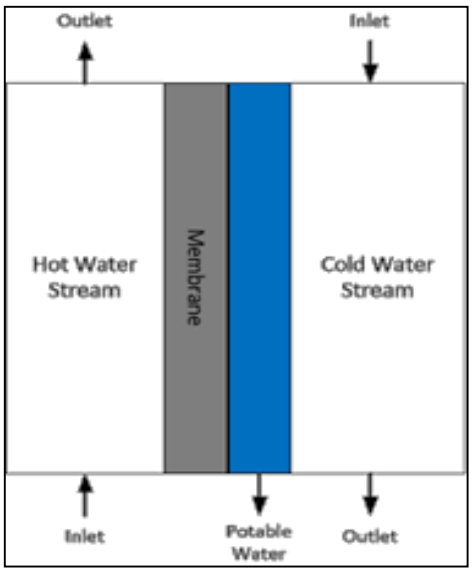

Figure4SGMD

Figure 5 DCMD Configuration

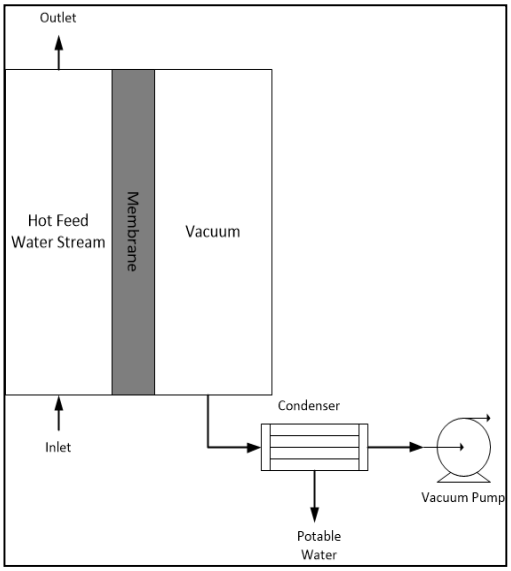

Figure 6 VMD Configuration

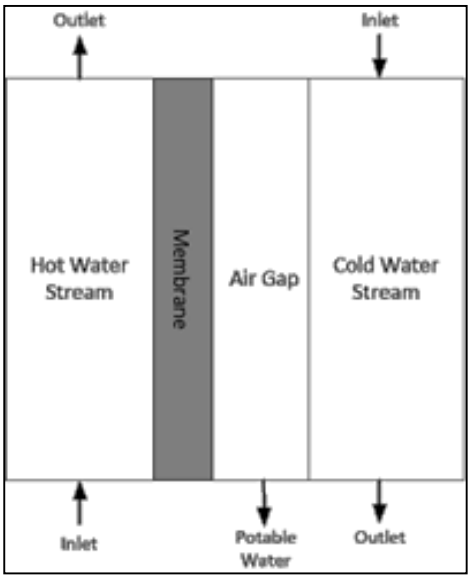

Figure 7- AGMD Configuration

Comparison of Membrane Distillation types

A comparison of the types of MD is given in the table 1

Table 1-Comparison of MD Techniques

MD Type	Advantages	Disadvantages
DCMD	1. Simple design 2. Heat can be recovered 3. High permeate flux	1. Large thermal energy loss 2. Large temperature and concentration polarization
AGMD	1. Low thermal energy loss 2. Heat can be recovered 3. Seawater can be used on permeate side	1. Mass transfer resistance due to air gap 2. Large footprint

SGMD	1. Low thermal energy loss 2. Increased mass transfer rate	1. Difficult heat recovery 2. Dealing with inert gate is complicated 3. Large condenser is required
VMD	1. High permeate flux 2. Low thermal energy loss 3. Small effect of temperature and concentration polarization	1. Membrane pore wetting is powerful 2. Heat recovery is difficult

Although maintaining a constant vacuum and hence a large pressure difference between the two sections of VMD module while ensuring leak proof operation is a challenge, yet the fact that VMD has a higher flux rate and high thermal efficiency as compared with other MD types is the reason that VMD was chosen for this project.

Membrane Characteristics

Material

The MD process uses hydrophobic microporous membranes. These membranes are made of polyvinylidene fluoride (PVDF), polypropylene (PP) or polytetrafluoroethylene (PTFE). [9,10]

Liquid Entry Pressure

In the MD process, the feed must not enter the membrane for which the applied pressure must not exceed the Liquid Entry Pressure (LEP) which is the preesure at which the feed enters the membrane. Membranes that have high surface tension, low surface energy, small pore size, and a high contact angle possess a high LEP value. For VMD, a small pore size is used to ensure a large LEP.

Membrane Thickness

The permeate flux in MD has an inverse relationship with the membrane thickness. As the thickness increases, the resistance to mass transfer increases while the resistance to heat transfer decreases. Lagana et al [11] concluded theoretically that the optimum membrane thickness lies between 30-60 μm.

Membrane Porosity and Tortuosity

Membrane porosity refers to the percentage of volume occupied by pores to the total membrane volume. The greater the porosity, the greater the evaporation surface area. Generally a membrane with higher porosity has a greater mass flux and a lower heat loss due to conduction. Membrane porosity in MD varies from 35-80 % [18].

Tortuosity is the extent to which the pore structure deviates from the cylindrical shape. A higher value of tortuosity results in a lower permeate flux.

Mean Pore Size and Pore Size Distribution

In MD systems, membranes with average pore size between 100 nm and 1 μm are usually used. [18] Permeate flux increases by increasing pore size [18]. Scanning Electron Microscopy (SEM) can be used to study the top and bottom section and the cross section of a membrane to estimate porosity, pore size, morphology, surface quality and pore size distribution. Atomic force microscopy, bubble point with gas permeation, and permeability method can also be used to estimate pore size distribution, average pore size and porosity. [19]

Applications of Vacuum Membrane Distillation

VMD has been used for a multitude of applications. Table 2 summarizes these application areas:

Table 2- Application of VMD

Ref.	Purpose	Solution
[20]	Removal	Toluene and benzene removal from water
[21]		Separation of alcohols, VOCs and trace gases from aqueous solutions (water)
[22]		Separation of chloroform dilute aqueous streams
[23]		Removal of volatile halogenated organic compounds
[26]		Inhibitors from lignocellulosic hydrolyzates
[27]		Ethanol from fermentation broth
[28]	Concentration	Aqueous sugar containing solution during drink production
[29]		Solution concentration and crystallization
[30]		Better flavoured and coloured juices and also retrieval of volatile aroma compound
[34]	Treatment	Highly strenuous solutions of salts
[35]		Treatment of waste water

[36] [37]		Treatment of water that are in mines Treatment of waste that is produced during radioactive processes
[39] [40]	Purification	Purification of dilute solutions Purification of (AS) arsenic containing water
[41]	Desalination	Desalination of sea water and others like brackish

Membrane Distillation Modules

Spiral Wound Membrane

Flat sheet membrane and spacers are enveloped and rolled around a perforated central collection tube. The feed moves across the membrane surface axially, while the permeate flows radially towards the center and leaves through the collection tube. The spiral wound membrane has good packing density, average tendency to fouling and acceptable energy consumption.

Hollow fibre

The hollow fibre module, which has been used in MD, has thousands of hollow fibres bundled and sealed inside a shell tube. The feed solution flows in the fibres and the permeate is collected on the outside of the membrane fibre (inside-outside), or the feed solution flows from outside the hollow fibres and the permeate is collected inside the hollow fibre (outside-inside). Hollow fibre module has very high packing density and low

energy consumption. On the other hand, it has high tendency to fouling and is difficult to clean and maintain.

Tubular Membrane

The membrane is cylindrical and inserted between the two cylindrical chambers. This configuration is easy to clean, less prone to fouling, and has a large effective area.

Plate and Frame

The membrane and spacers are placed between two flat plates. It is used extensively in laboratory studies because it is easy to clean.

Operating Conditions and their Effect on Permeate Flux

In this section the parameters which affect the performance of VMD modules will be discussed.

Feed Temperature

When the temperature of feed water solution is increased, it results in an increased permeate concentration/flux. The table 3 shows results from some experimental studies on VMD and effect of temperature on flux.

Table 3- Effect of temperature on permeate flux

Ref.	Variation in T	Effect on flux
[45]	Increase from 329-345*C	Increase from 2.976-10.89 $kg/m^2.hr$
[46]	Increase from 310.2-319.2 K	Increase from 8.2-13.8 $kg/m^2.hr$
[47]	Increase from 50-70 *C	Increase from 4.6-9.5 $kg/m^2.hr$

Feed Concentration

An increase in feed concentration has a negative effect on permeate flux as shown by table 4.

Table 4- Effect of temperature on permeate flux

Ref.	Variation in T	Effect on flux
[45]	Increase from 10-26 g/L	Decrease from 11.2-9 kg/m^2.hr
[46]	Increase from 58.4 -175.2 g/L	Decrease from 13.8-12 kg/m^2.hr
[47]	Increase from 5-20 g/L	Decrease from 8.42-6.82 kg/m^2.hr

Feed velocity

An increase in fed velocity is accompanied by an increase in permeate generation as shon by table 5. The increase in feed velocity creates turbulence and decreases effect of temperature and concentration polarization. This enhances the flux generation.

Table 5- Effect of temperature on permeate flux

Ref.	Variation in feed velocity	Effect on flux
[45]	Increase from 10-80 L/hr	Increase from 5-11 kg/m^2.hr
[46]	Increase from 50-100 L/hr	Increase from 13.8-16 kg/m^2.hr
[48]	Increase from 19.9-33.2 L/hr	Increase from 4-6 kg/m^2.hr

Vacuum Pressure

The pressure difference across the membrane has a profound effect on permeate flux. An increase in pressure difference creates a stronger driving force and thereby has a positive effect on production of permeate flux. Table 6 summarizes findings from some experimental work carried out in the past.

Table 6- Effect of temperature on permeate flux

Ref.	Variation in vacuum	Effect on flux
[45]	Increase in vacuum from 69-83 kPa	Increase from 1.9-11 $kg/m^2.hr$
[49]	Reduction in downstream pressure from 17-5 kPa	Increase from 1.2-2 $kg/m^2.hr$
[48]	Reduction in downstream pressure from 70-30 kPa	Increase from 6-9.5 $kg/m^2.hr$

CHAPTER 3: METHODOLOGY

Mathematical Modelling:

In a VMD process, heat and mass transfer processes occur simultaneously. For analysis, the system is divided into different sub-systems: (i)The bulk feed solution, (ii) the feed boundary layer (adjacent to the membrane), (iii) membrane, and (iv) permeate bulk region (figure 8). The boundary layer is absent next to the membrane in the permeate side because of the presence of low pressure. It enables a higher flux in VMD as compared to DCMD, AGMD, and SGMD. [50,9]

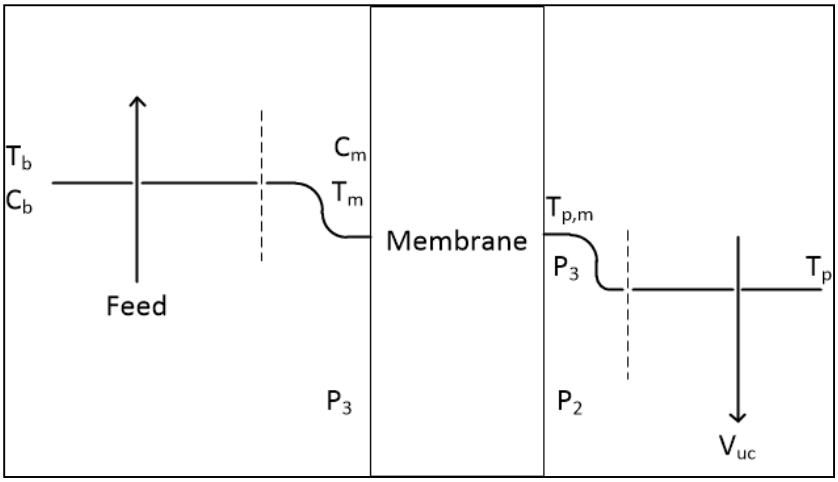

Figure 8- Different sub-systems in VMD and depiction of polarization of temperature and concentration

Mass Transfer:

The transfer of mass across the membrane in a MD process can be explained with the aid of kinetic theory of gases. The mass transfer is explained with the help of one or a combination of more than one of the following models: (i) Knudsen flow model, (ii) Viscous flow model, and (iii) Ordinary Molecular Diffusion model. [50,9]

The Ordinary Molecular Diffusion model is applied when the mean free path of the gas molecules is at least one order larger than the pore diameter of the porous media. Laws of

diffusion developed by Fick are used to define a relationship between the diffusion flux and the concentration gradient. The flux depends on a number of factors including the molar fraction of gas species and bulk diffusivity. For porous media as in the case of hydrophobic membrane, porous media factors are introduced to account for the porosity of the medium.

The Viscous Flow model (Hagen–Poiseuille flow) describes the drop in pressure for a Newtonian incompressible fluid flowing through a long cylindrical pipe of constant cross section when the flow is laminar. The pressure drop depends on the dynamic viscosity, length of pipe, flow rate, and pipe radius. A more complex model such as Darcy–Weisbach equation is applied to describe flow where the viscous flow model fails.

The Knudsen Flow model is applied when the molecular mean free path is much greater than the diameter of the pore in which the diffusing molecule resides. The molecule collides with the wall more often than colliding with other molecules. According to this model, the mass transfer depends on the temperature, cylindrical pore diameter, and molecular mass of the diffusing specie. The Knudsen number is defined by equation 1

$$\text{Kn} = \frac{\lambda}{d}$$

$$\lambda = \frac{k_{b*T}}{\sqrt{2} * \pi * d^2 * P}$$

If the Kn >> 10, the collisions between the gas molecules and the porous electrode are more dominant than the collisions between gas molecules. The molecular and viscous diffusion become negligible and Knudsen model is applied. When, 0.1 < Kn < 10, all three mechanisms are required to describe the mass transfer. When, the Kn << 0.1, the

collisions between gas molecules becomes dominant. Knudsen type diffusion become insignificant while the molecular and viscous diffusion become important. The resistances to mass transfer are further discussed in the following paragraphs.

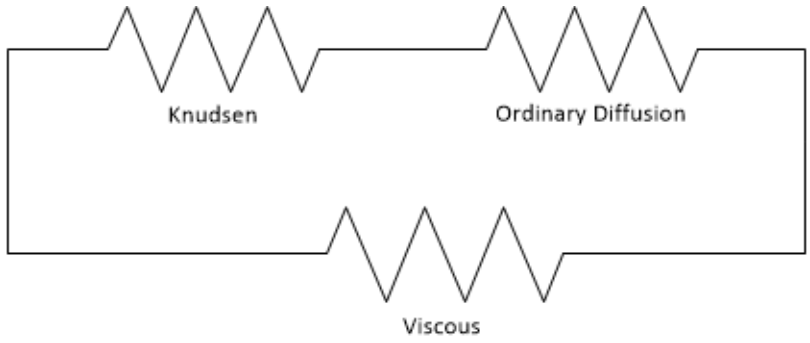

Figure 9- Resistances to mass transfer in MD

When the liquid water adjacent to the membrane vaporizes and crosses the membrane towards the vacuum side, the salt concentration increases resulting in a difference of concentration between the bulk feed solution and the solution adjacent to the membrane. These salt ions will accumulate near the membrane pores and stop water vapors from entering the membrane pores. In other words, the volatile species needs to diffuse around non-volatile species. According to Bandini and Sarti [51], this resistance is insignificant for solution that involves pure water and dilute salt solution. This resistance becomes important when Volatile Organic Compounds (VOCs) are present in the solution. Owing to absence of VOCs in the solution to be used in this study, this resistance will be neglected here.

Before application of vacuum, the pores of the membrane contain non condensable gases like N_2 and O_2 . These gases remain in the pores and present opposition to the water vapors as they move towards the vacuum side. Once the low vacuum ai applied, the partial pressure of these non condensable gases becomes very small as compared to the water vapor molecules inside the pores of the membrane. Thus, this resistance becomes very small and is not accounted for. In VMD, the gas molecule may collide with other molecules or with the membrane walls. Since the amount of air inside the pores is very

low, the molecule-molecule collisions between water and air are insignificant, and hence the ordinary molecular diffusion model is not used to describe mass diffusion.

For a typical VMD process with 0.1-0.2 μm pore size and a mean free path for water several times greater than the pore size (2.8 μm at 30 °C) for which Kn is 14-28 and hence the Knudsen flow model is used to describe mass transport because the molecule collides with the wall more often than colliding with other molecules. This type of resistance is considered the main resistance to mass transfer in VMD. If the pore size had been greater than the mean free path, the viscous flow model would have been better at describing the mass transport because the viscous forces between the water vapor molecules would have been a key factor for the description of flow. For these reasons, the Knudsen type diffusion is used to describe mass transport in this study.

For the Knudsen type diffusion, the water vapor flux J across the membrane depends on the transmembrane water vapor pressure difference ΔP according to the following equation [9,16,19,46,52]:

$$J=B*\Delta P=B*(Pm(Tm,xsalt)-P\mathrm{v})$$

$$B = 1.064\left(\frac{r\cdot\varepsilon}{\delta\cdot t}\right)\sqrt{\left(\frac{M}{RT}\right)}$$

It should be noted that an average value for the pore size is used in the expression. In an actual membrane, all pores are not of the same size.

The water vapor pressure on the membrane surface, P_m, depends on the temperature on the membrane surface T_m by the Antoine equation eq (3):

$$P_m(Tm, x_{salt}) = \exp(23.1964 - \frac{3816.44}{T_m - 46.13})$$

When writing (3), the curvature of the liquid/vapor surface is assumed to have negligible effects on the equation as compared to the flat surface state. Equation (3), however, does not incorporate effect of solute (dissolved salt) on the water vapor pressure. According to Raoults's law, the vapor pressure of a pure substance (water) and vapor pressure of a water-salt solution are different. To account for the effect of the solute, equation (3) is modified as [53]:

$$P_m(Tm, x_{salt}) = \exp(23.1964 - \frac{3816.44}{T_m - 46.13})(1 - x_{salt})(1 - 0.5x_{salt} - 10x_{salt}^{2})$$

It should be noted here that the temperature at the membrane surface T_m differs from the temperature of the bulk feed solution, T_b. When water evaporates near the membrane, the local temperature drops. Thus, T_m is less than T_b. This creates a temperature gradient between the bulk feed solution and the solution adjacent to the membrane referred to as temperature polarization in literature [16,19,46,52,53].

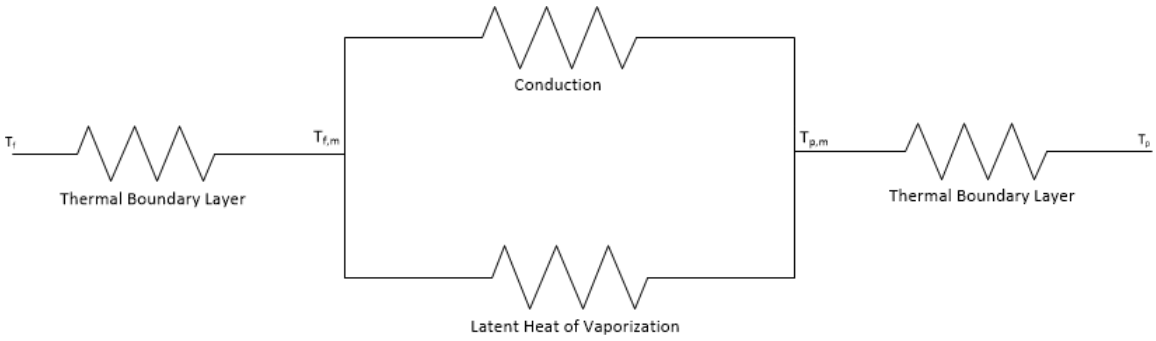

Figure 10- Resistances to Heat transfer in MD

Heat Transfer

As mentioned earlier, the mass transfer and heat transfer processes are coupled in MD. Energy is first transported as heat from the bulk feed solution to the feed boundary layer region due to the temperature gradient. Then it is transported across the membrane. The heat transfer across the membrane is made up of two parts: one part is associated with the latent energy of the water vapor molecules and the other is heat transfer through the membrane material.

In a VMD process, due to very low pressure on permeate side, the conductive heat across the membrane material is negligible and therefore the energy associated with water vapor is considered only. [19,50]

The heat transferred Q is defined as:

$$Q=h*(Tb-Tm)$$

Where h is the convective coefficient of heat transfer. It depends on the Reynolds number and fluid properties. At steady state, the energy balance for the VMD process can be written as:

$$h*(Tb-Tm)=J*Hv=Bm*Hv*\Delta P$$

$$h=\frac{k_m*N_u}{d_h}$$

The Nusselt number is calculated using:

$$Nu=1.86*(Re*Pr*\frac{d_h}{l})\ \ Laminar\ flow\ Re<2100$$

$$Nu=0.023*(R_e{}^{0.8}*P_r{}^{0.33})\ \ Turbulent\ flow\ Re>4000$$

It is important to inform the reader that the heat transfer coefficients are usually estimated, in MD studies, from empirical correlations depending on the flow regime. Since these correlations have been developed for non-porous and rigid heat exchangers, their use for modeling VMD does not mimic the experimental conditions exactly since membranes are neither rigid nor non-porous. However, they have been exhaustively applied to model VMD in literature and their application yields satisfactory results [16,19]. Therefore, they have been employed in this study as well.

Temperature Polarization Coefficient:

For a DCMD configuration, Schofield et al [54] have defined the TPC as the ratio of temperature differences at the membrane interface and the bulk feed solutions:

$$TPC=\frac{Tmf-Tmp}{Tbf-Tbp}$$

Where T_{mf}, T_{mp}, T_{bf}, and T_{bp} are the temperatures at the membrane interface at the feed side, temperatures at the membrane interface at the permeate side, temperatures of the bulk solution at the feed side, and temperatures of the bulk solution at the permeate side respectively

When TPC value approaches 1, it indicates high heat transfer convective coefficients and the bulk temperatures can be used to calculate the water vapor flux without producing considerable error while a value close to 0 indicates that the temperatures at the membrane interface on either sides should be used to compute flux.

For VMD, three definitions have been used in literature to calculate TPC [52]. Some authors [46,55,56] have defined it as:

$$TCP = \frac{Tm}{Tb}$$

In this case, TCP approaches zero as T_m approaches 0. A higher value (close to 1) will indicate a decreased effect of polarization. On the other hand a smaller value (closer to 0) will indicate a greater polarization effect.

Bandini et al. [51] defined TCP as:

$$TCP = \frac{Tb - Tm}{Tb - Tv}$$

Where T_v is the temperature at the vacuum side. When the heat transfer coefficient is high, TPC will approach 0 for this definition while for a low heat transfer coefficient TPC will approach 1. Thus, it represents the relationship between heat transfer and the resultant temperature gradient between bulk solution and solution at membrane interface.

Some authors [58,59] modified the definition by Bandini to define TPC as:

$$TCP = \frac{Tm - Tb}{Tb - Tv}$$

VMD Module Design:

Material:

Material that has been selected to manufacture the module is acrylic. Because the following two issues would be likely encountered during operation:

- Water leaking out of the system
- Air leaking into it

By making the module using acrylic, these issues (if they do occur) can be located easily. In addition to this, acrylic offers high machinability, reasonably high strength and is lighter compared to metals.

Module Design:

Following issues needed to be kept in mind when the module was being designed

- It had to be sized according to the available membrane size.
- It needs to be easily manufacturable so that the manufacturing costs less are low and the process can be completed in the available time.
- Maximum area of the membrane needs to be utilized for maximum permeate
- Water flow needs to be designed suchthat there are no dead-zones in the system
- As the membrane is not easily acquirable, it needs to be protected during operation.
- The design needs to be strong enough to withstand the negative pressure being created by the vacuum pump.
- As the evaporation process is vital for any flux to be obtained, it needs to be facilitated by the design.

A rendering of module design is shown in figure(13). The top and bottome plates are made of acrylic. A membrane with pores has been shown at the centre

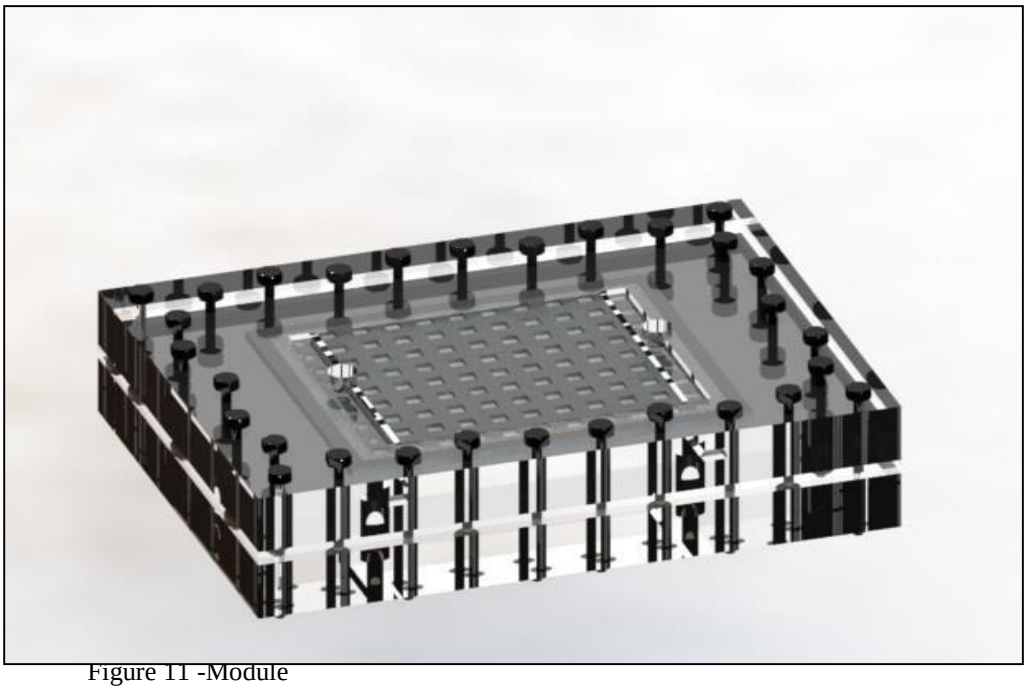

Figure 11 -Module

Design of Shell and Tube Heat exchanger:

A shell and tube heat exchanger must satisfy the process requirements with the allowable pressure drops. The design should be as:

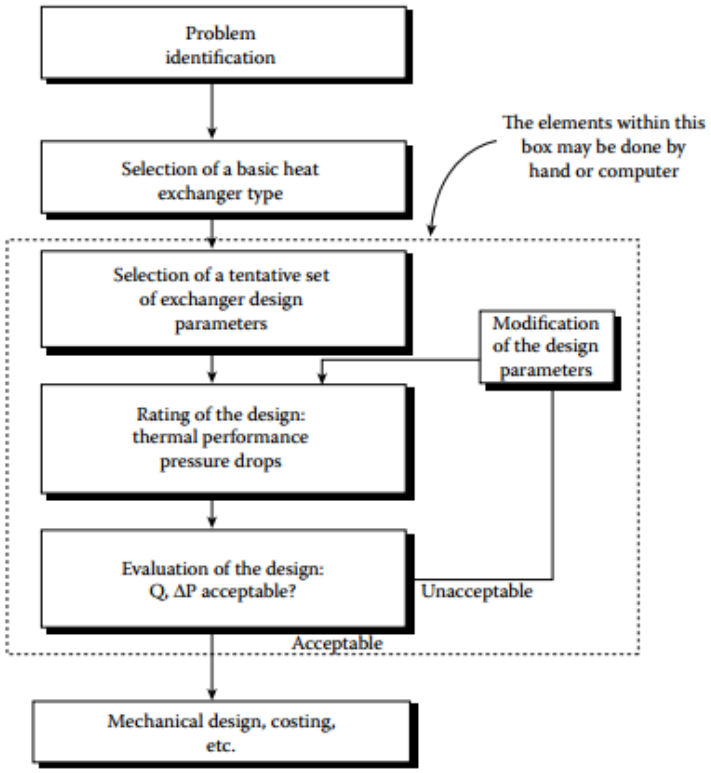

Figure 12- Heat exchanger design steps

Design steps

- Assume tube diameter, BWG (Birmingham Wire Gauge) and tube length.
- Assume fouling factor for both inside and outside tubes.
- Assume material of construction for tubes.

Table 7 Material Properties

Metal	Temperature (°C)	k_w(W/m°C)
Aluminium	0	202
	100	206
Brass	0	97
(70 Cu, 30 Zn)	100	104
	400	116
Copper	0	388
	100	378
Nickel	0	62
	212	59
Cupro-nickel (10 per cent Ni)	0–100	45
Monel	0–100	30
Stainless steel (18/8)	0–100	16
Steel	0	45
	100	45
	600	36
Titanium	0–100	16

- Assume the temperatures that are required according to application and then find the mass flow rate of other stream with known mass flow rate of one stream by using heat duty equation:

$$q=m_c\, cp_c\, (T_{c\ out}-T_{c\ in})=m_h\, cp_h\, (T_{h\ out}-T_{h\ in})$$

- Find log mean temperature difference.

  For counter current: $$LMTD=\frac{(T_{hi}-T_{co})-(T_{ho}-T_{ci})}{\ln\frac{(T_{hi}-T_{co})}{(T_{ho}-T_{ci})}}$$

  For co current: $$LMTD=\frac{(T_{hi}-T_{ci})-(T_{ho}-T_{co})}{\ln\frac{(T_{hi}-T_{ci})}{(T_{ho}-T_{co})}}$$

- Obtain temperature coefficient factor.

$$R=\frac{(T_1-T_2)}{(t_2-t_1)} \qquad S=\frac{(t_2-t_1)}{(T_1-t_1)}$$

  Following charts are used for configurations as:

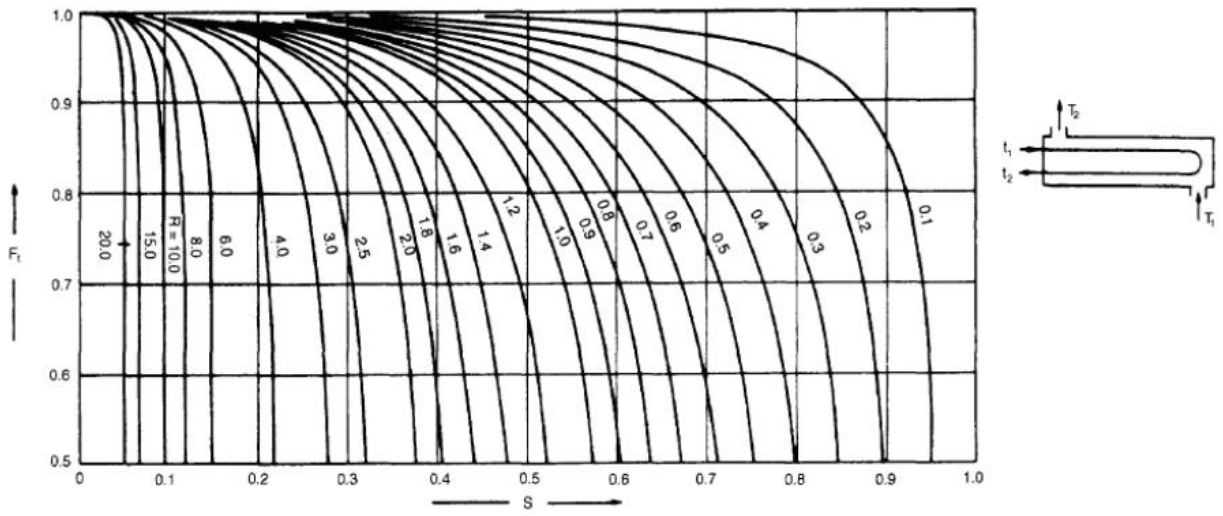

Figure 13- One shell pass, two or more even tube passes.

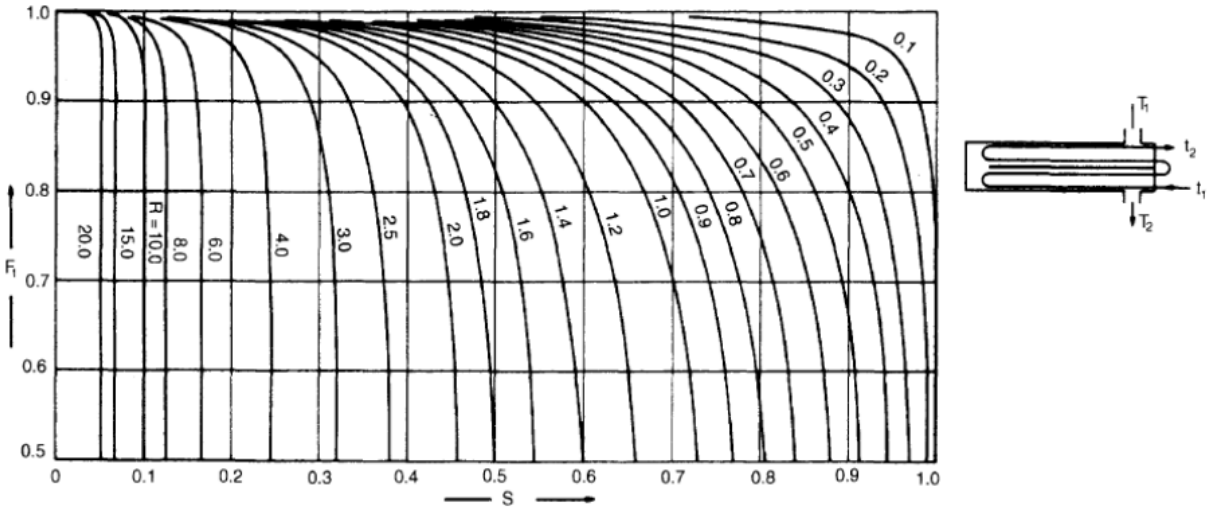

Figure 14-Two shell passes, four or multiples of four tube passes

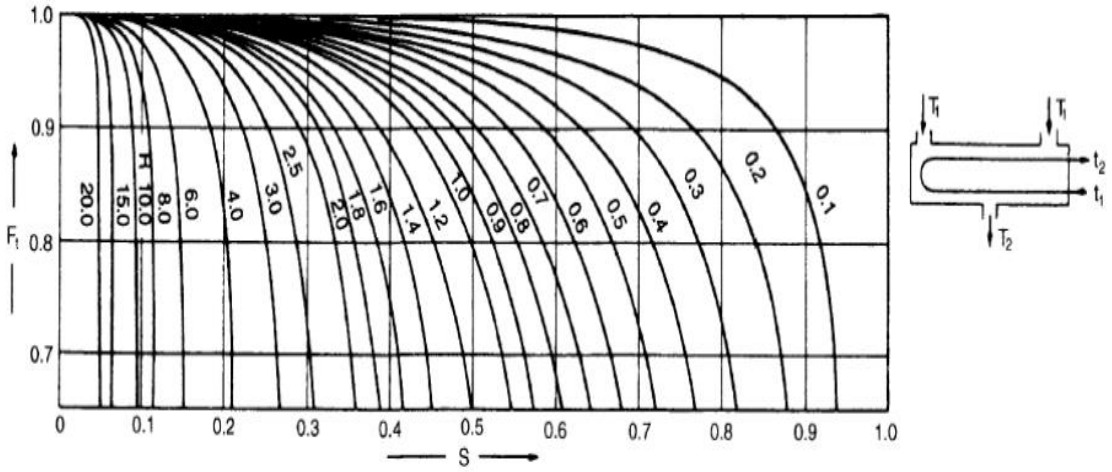

Figure 15-Divided flow shell, two or more even tube passes

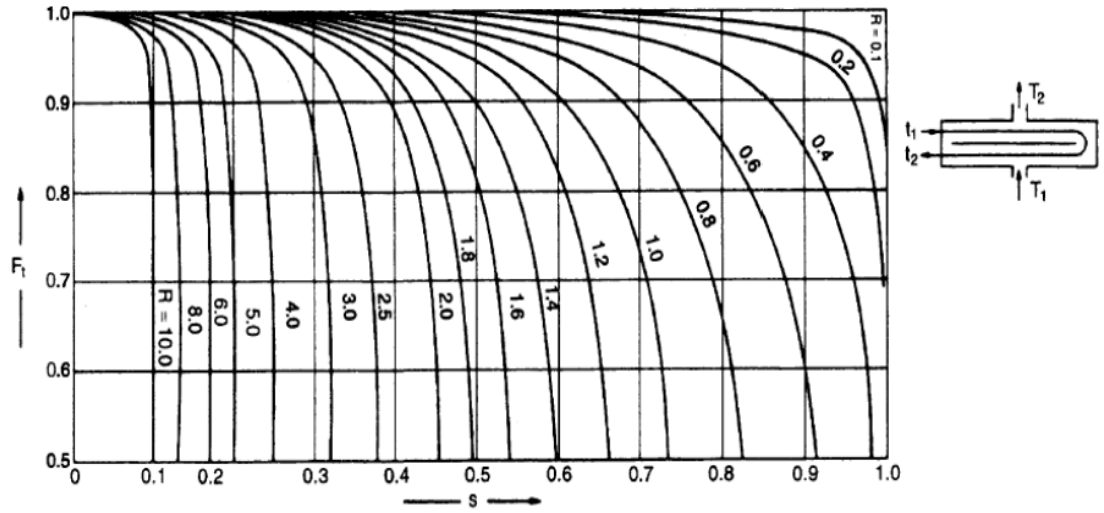

Figure 16- Split flow, two tube pass.

- Calculate mean temperature difference by:

$$DT_m = F*LMTD$$

- Assume overall heat transfer coefficient from table given below:

Table 8 Fluid Properties

Shell and tube exchangers		
Hot fluid	Cold fluid	U (W/m^2°C)
Heat exchangers		
Water	Water	800–1500
Organic solvents	Organic solvents	100–300
Light oils	Light oils	100–400
Heavy oils	Heavy oils	50–300
Gases	Gases	10–50
Coolers		
Organic solvents	Water	250–750
Light oils	Water	350–900
Heavy oils	Water	60–300
Gases	Water	20–300
Organic solvents	Brine	150–500
Water	Brine	600–1200
Gases	Brine	15–250
Heaters		
Steam	Water	1500–4000
Steam	Organic solvents	500–1000
Steam	Light oils	300–900
Steam	Heavy oils	60–450
Steam	Gases	30–300
Dowtherm	Heavy oils	50–300
Dowtherm	Gases	20–200
Flue gases	Steam	30–100
Flue	Hydrocarbon vapours	30–100
Condensers		
Aqueous vapours	Water	1000–1500
Organic vapours	Water	700–1000
Organics (some non-condensables)	Water	500–700
Vacuum condensers	Water	200–500
Vaporisers		
Steam	Aqueous solutions	1000–1500
Steam	Light organics	900–1200
Steam	Heavy organics	600–900

- Calculate provisional area

$$A=\frac{q}{U.DT_m}$$

- Find number of tubes

$$N_t=\frac{A}{\pi\, d_o L}$$

- Calculate pith diameter and bundle diameter

$$P_t=1.25\ d_o \qquad D_b=d_o\ (\frac{N_t}{K})\text{^}\ \frac{1}{n_1}$$

Where k and n are obtained through following table:

Table 9, No of passes

Triangular pitch, $p_t = 1.25d_o$					
No. passes	1	2	4	6	8
K_1	0.319	0.249	0.175	0.0743	0.0365
n_1	2.142	2.207	2.285	2.499	2.675
Square pitch, $p_t = 1.25d_o$					
No. passes	1	2	4	6	8
K_1	0.215	0.156	0.158	0.0402	0.0331
n_1	2.207	2.291	2.263	2.617	2.643

- Assume bundle clearance diameter BDC and calculate Shell diameter

$$D_s=D_b+BDC$$

- Calculate baffle spacing

$$BS=0.4\ D_s$$

- Calculate area for cross flow

$$A=\frac{(Pt-do\ )D_sB_s}{Pt}$$

- Calculate shell side mass velocity

$$G_s=\frac{shell\ side\ mass\ flowrate}{A_s}$$

- Calculate shell equivalent diameter

For square pitch $d_e=\frac{1.27}{d_o}(p_t^2-0.785d_o^2)$

- Calculate shell side Reynold number, Prandtl number and shell side heat transfer coefficient

  Re=$\frac{G_s d_e}{\mu}$ Pr=$\frac{\mu C_p}{k}$ Nu=j_h Re $Pr^{1/3}(\frac{\mu}{\mu_w})^{0.14}$

  Where j_h can be found by the chart below

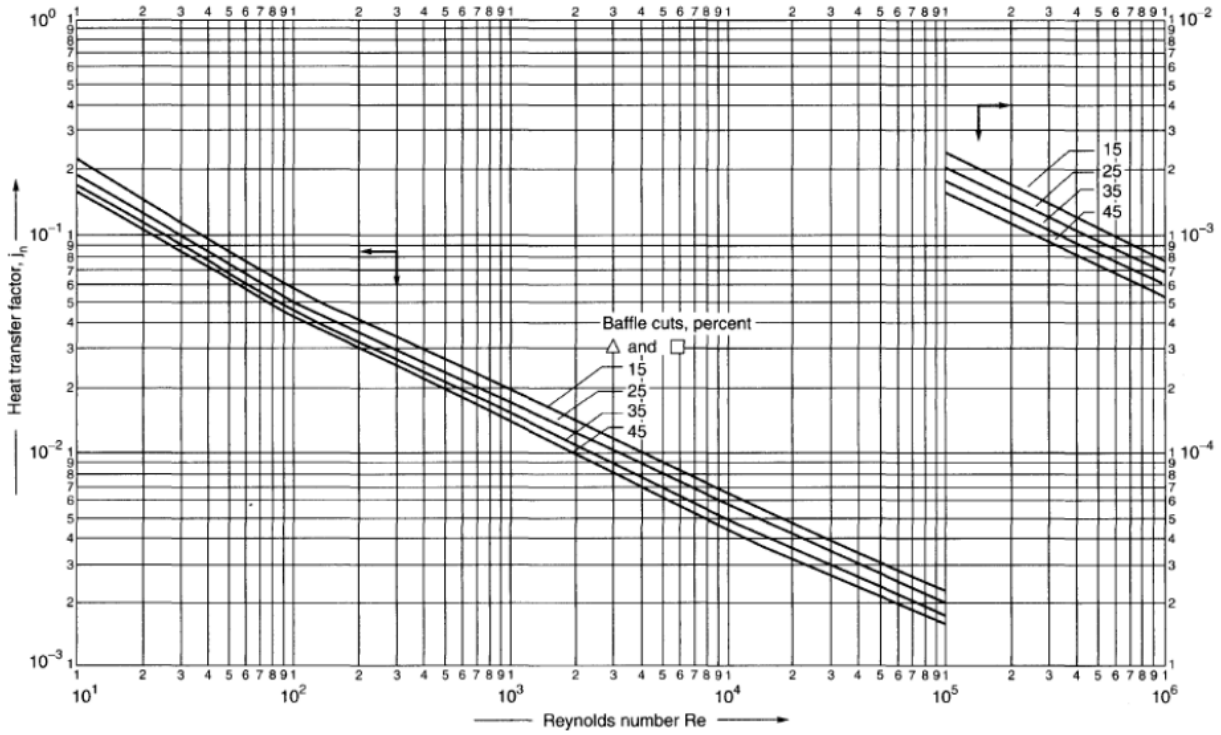

Figure 17- Chart

Calculate pressure drop in shell

$$\Delta P_s = j_f (\frac{D_s}{d_e})(\frac{L}{l_b})(\frac{\rho \mu_s \hat{} 2}{2}) (\frac{\mu}{\mu_w})^{0.14}$$

where j_f can be found by chart

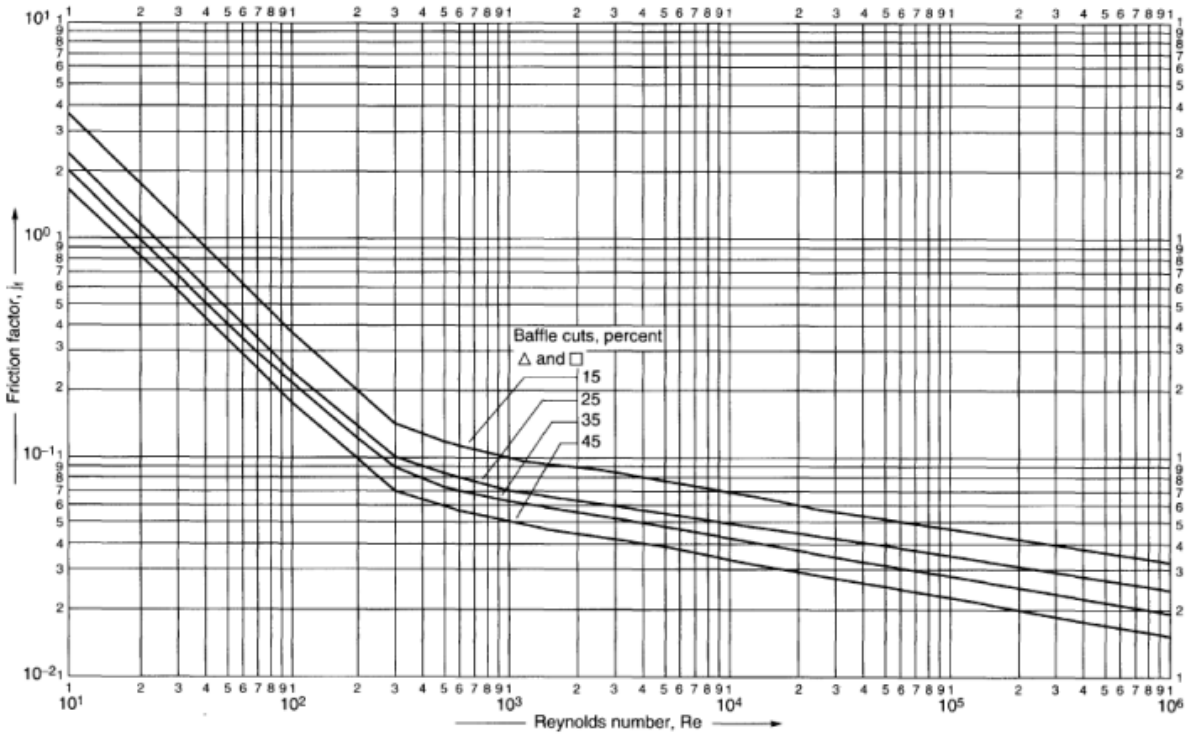

Figure 18

- Calculate tube per pass by dividing number of tubes by number of passes and also calculate tube side mass velocity

$$G_m=\frac{tube\ side\ flowrate}{\frac{\pi {d_i}^2}{4} N_{tpp}}$$

- Calculate tube side velocity by dividing tube side mass velocity by density and then calculate Reynold and Prandtl number.

$$Re=\frac{\rho d_i v}{\mu} \qquad Pr=\frac{\mu C_p}{k}$$

- Calculate tube side heat transfer coefficient

$$Nu=j_h\ Re\ Pr^{1/3}\left(\frac{\mu}{\mu_w}\right)^{0.14}$$

- Calculate overall heat transfer coefficient

$$U=\left(\frac{1}{h_i}+\frac{d_i \ln\left(\frac{d_o}{d_i}\right)}{2k}+\frac{d_i}{d_o h_o}+\frac{d_i R_{fo}}{d_o}+R_{fi}\right)^{-1}$$

- Now check that the calculated overall heat transfer coefficient comes out to be close to our initial guess overall heat transfer coefficient and if not then use this calculated and repeat the procedure until both overall transfer coefficient comes to be close.

Baseline Parameters:

Table 10 Heat exchanger parameters

Parameters	Values
Inlet temperature for hot fluid	90
Outlet temperature for hot fluid	60
Inlet temperature for cold fluid	30
Outlet temperature for cold fluid	70
Mass flow rate through tube	14.88375
Thermal conductivity	46
BWG	18

HAPTER 4: RESULTS AND DISCUSSIONS

Results of Mathematical Modeling

i. Model Validation

The mathematical modeling was validated using parameters published in an experimental study of VMD by Naidu et al. [46]. The equations were solved using software packages MATLAB and MAPLE. The code is present in Appendices 1 and 2. Table (8) shows parameters used as inputs for the model.

Table 11- Operating parameters from Naidu et al. [46]

Parameter	**Value**
Membrane material	Polytetrafluoroethylene (PTFE)
Effective membrane area (m^2)	0.16
δ (μm)	179
ω (%)	70-75
r (μm)	0.2
Feed velocity v (m/s)	1.1 and 2.2
Feed flow rate $\dot{V}$ (L/hr)	50 and 100
Bulk feed temperature Tb (K)	310.2, 313.7, and 319.2
Pressure on vacuum side Pv (kPa)	4.5

The model was used to calculate Temperature Polarization Coefficient (TPC) and flux J at the same conditions as in the experimental study using the algorithm shown in figure (15). The results of the experimental study and mathematical model are compared in the tables (9-11). The mathematical model was solved for different temperatures of feed water solution 310.2 K, 313.7 K, and 319.2 K at two different feed velocities: 1.1 m/s at a flow rate of fifty L/hr and 2.2 m/s at a flow rate of hundered L/hr.

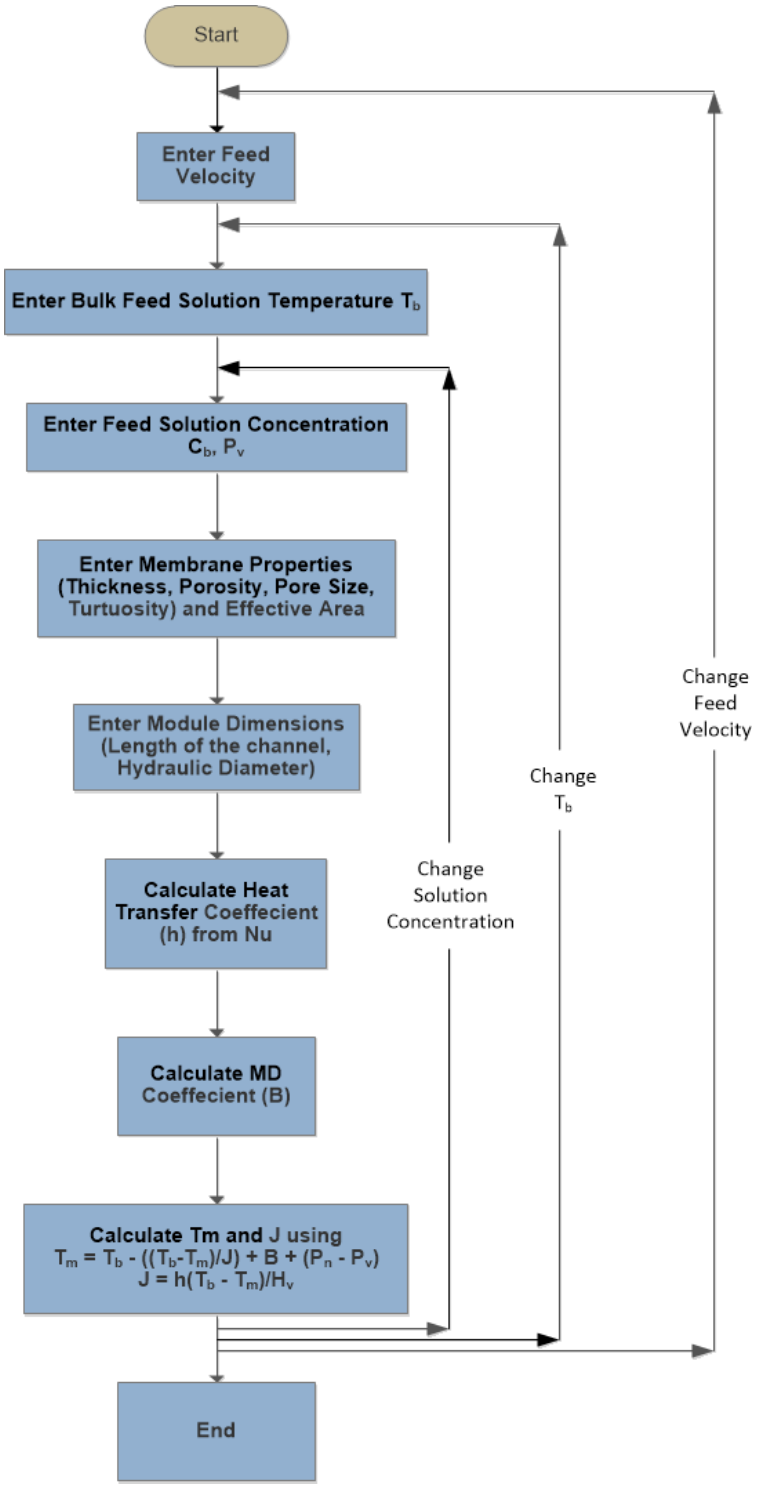

Figure 19- Algorithm used for Mathematical Modeling

Table 12- Comparison between J results for model presented here and the experiment by Naidu et a. [46] for v=1.1 m/s

T_b (K)	**Concentration (M)**	**Predicted Flux, J_{th} (L/hr*m^2)**	**Exp. Flux, J_{exp} (L/hr*m^2)**	**% Difference** $\frac{J_{th}-J_{exp}}{J_{th}}*$
310.2	1	8.46	8.5	-0.47
	2	8.19	8	2.38
	3	7.87	7	12.43
313.7	1	10.19	9.75	4.51
	2	9.86	9	9.56
	3	9.47	7.8	21.41
319.2	1	13.39	13.7	-2.26
	2	12.96	12.5	3.68
	3	12.49	11.6	7.67

The comparison of values of flux J between the model and experiments in tables (9) and (10) shows that the model can be successfully applied to predict the flux for different operating conditions of concentration and bulk temperature with <10% error for most scenarios.

The TPC values for the model are calculated using (T_f / T_b). The values are tabulated in table (11) against those mentioned in [46]. Only values corresponding to 50 L/hr volume flow rate at different values of concentration and bulk feed temperature are used for comparison since Naidu et a. [5] have not used the same values of bulk temperatures in the case of 100 L/hr simulation.

Table 13- Comparison between J results for the present model and the experiment by Naidu et a. [46] for v=2.2 m/s

T_b (K)	Concentration (M)	Predicted Flux, J_{th} (L/hr*m2)	Exp. Flux, J_{exp} (L/hr*m2)	% Difference $\frac{J_{th}-J_{exp}}{J_{exp}} * 100$
310.2	1	8.96	9.5	-5.68
	2	8.64	9	-4
	3	8.28	7.75	6.84
313.7	1	10.87	11.5	-5.48
	2	10.49	10.5	-0.095
	3	10.07	9.2	9.46
319.2	1	14.47	15.8	-8.42
	2	13.99	14.8	-5.47
	3	13.45	14	-3.93

Table 14- Comparison between TPC results for the present model and the experiment by Naidu et a. [46] for v=1.1 m/s

T_b (K)	Concentration (M)	TPC_{th} (predicted %)	TPC_{exp} (exp. %)	% Difference $\frac{TPC_{th}-TPC_{exp}}{TPC_{exp}} * 100$
310.2	1	99.44	98.6	0.86
	2	99.46	98.8	0.67
	3	99.48	99	0.49
313.7	1	99.34	97.5	1.88
	2	99.36	97.8	1.59
	3	99.39	98	1.41
319.2	1	99.14	96.1	3.17
	2	99.17	96.6	2.67
	3	99.20	96.8	2.48

After validation of mathematical modeling, simulations are run for different operating conditions for current project specifications given in table 11. The membrane has been acquired from Sterlitech Corporation Ltd. USA. Its product code is QL822 and size is 200x250 mm. The membrane properties have been determined by the manufacturer.

Table 15- Specifications for current project

Parameter	**Value**
Membrane material	Polytetrafluoroethylene (PTFE)
Effective membrane area (m^2)	0.0336
δ (μm)	165
ω (%)	70-75
r (μm)	0.2
Feed velocity v (m/s)	various
Feed flow rate $\dot{V}$ (L/hr)	various
Bulk feed temperature Tb (K)	various
Pressure on vacuum side Pv (kPa)	various
Room Temperature (K)	283

ii. Effect of feed water concentration

An increase in feed water concentration has a negative effect on permeate flux. For example, when the concentration is increased from 0.25 M to 1.0 M at 318 K and flow rate of 50 L/hr, the permeate flux decreases from 20.80 L/m^2.hr to 20.50 L/m^2.hr which is a decrease of 1.44 %. A similar trend can be seen for other operating conditions as shown in figure 16 and 17 and in tables 12 and 13.

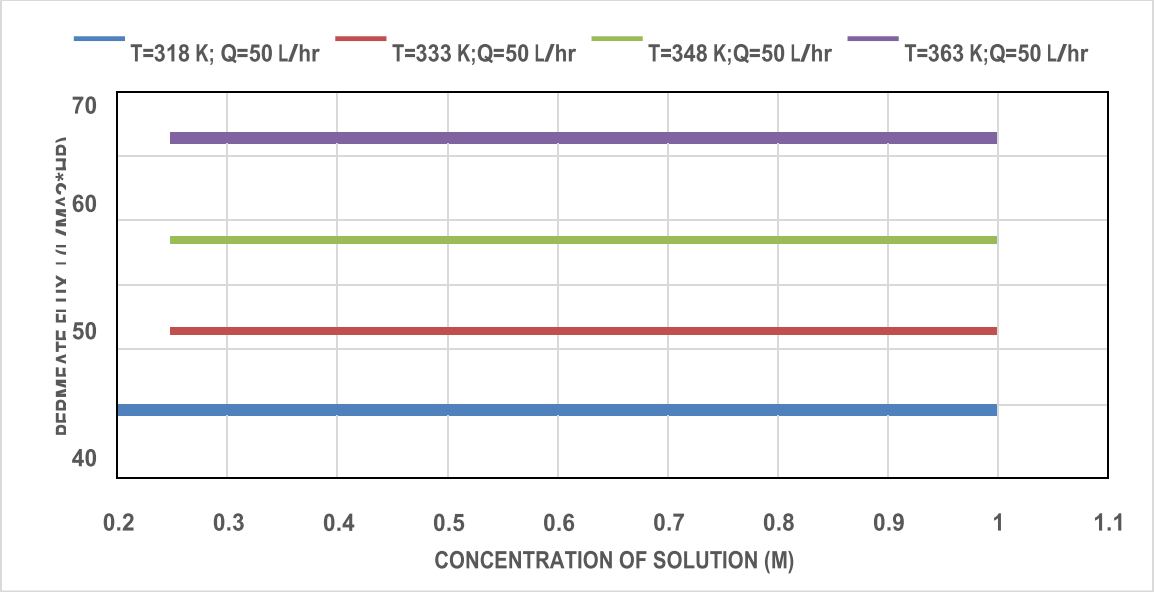

Figure 20- Permeate flux as a function of solution concentration for different values of temperature for feed flow rate of 50 L/hr

This decreases in flux can be explained on the basis of resistance offered by the non-volatile salt ions to the volatile water vapors during mass transfer. The higher concentration decreased the vapor pressure of water. An increased number of ions in the vicinity of the membrane hinders the movement of water vapors as they enter the membrane pores. This decrease in the driving force is responsible for the drop in flux.

Table 16- Change in flux with Tb and concentration for flow rate of 50 L/hr

T_b (K)	Molarity	Flux J ($L/m^2.hr$)	T_b (K)	Molarity	Flux J ($L/m^2.hr$)
318	0.25	20.80430504	348	0.25	47.18015
	0.5	20.70758385		0.5	47.02989
	0.75	20.60639287		0.75	46.87248
	1	20.50085002		1	46.70805
333	0.25	32.94788992	363	0.25	63.0585
	0.5	32.82282701		0.5	62.88632
	0.75	32.69187767		0.75	62.70587
	1	32.5551795		1	62.51729

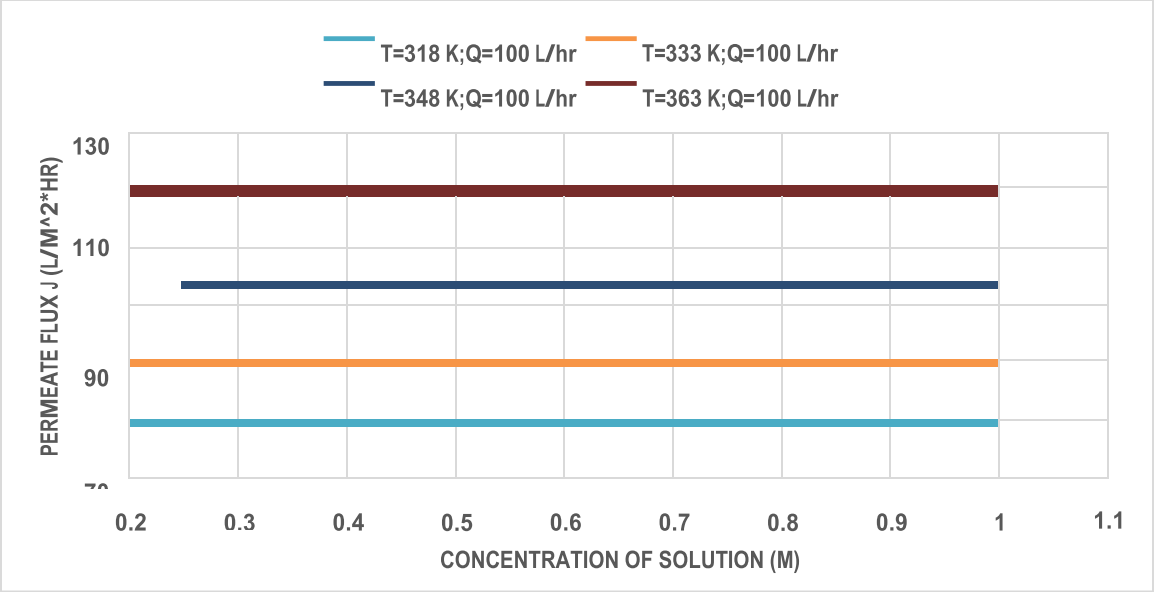

Figure 21- Permeate flux as a function of solution concentration for different values of temperature for feed flow rate of 100 L/hr

Table 17- Change in flux with concentration for different Tb (flow rate of 100 L/hr)

T_b (K)	Molarity	Flux J (L/m^2.hr)	T_b (K)	Molarity	Flux J (L/m^2.hr)
318	0.25	28.90600138	348	0.25	77.55811
	0.5	28.73984523		0.5	77.23502
	0.75	28.56629704		0.75	76.89693
	1	49.38714241		1	76.5442
333	0.25	50.15287199	363	0.25	110.3223
	0.5	49.90865314		0.5	109.9251
	0.75	49.65330362		0.75	109.5091
	1	49.38714241		1	109.0748

iii. Effect of feed water temperature

An increase in temperature of water solution entrance side (feed side), T_b, increases the flux on permeate side significantly. This is predicted by equations (1) and (4). The relationship between the temperature and the resultant vapor pressure is exponential

For example, when the feed solution temperature is increased from 318 K to 363 K for volume flow rate of 50 L/hr and concentration of 1 M, the permeate production increased from 20.80 L/m^2.hr to 62.5 L/m^2.hr which is an increase of 153%.

Table 18- Change in flux with Tb for various concentration (flow rate of 50 L/hr)

Molarity	T_b (K)	Flux J (L/m^2.hr)	Molarity	T_b (K)	Flux J (L/m^2.hr)
0.25	318	20.80430504	0.75	318	20.60639
	333	32.94788992		333	32.69188
	348	47.18014837		348	46.87248
	363	63.05849726		363	62.70587
0.5	318	20.70758385	1	318	20.50085
	333	32.82282701		333	32.55518
	348	47.0298946		348	46.70805
	363	62.88632269		363	62.51729

Table 19- Change in flux with Tb for various concentration (flow rate of 100 L/hr)

Molarity	T_b (K)	Flux J (L/m^2.hr)	Molarity	T_b (K)	Flux J (L/m^2.hr)
0.25	318	28.90600138	0.75	318	28.5663
	333	50.15287199		333	49.6533
	348	77.55811204		348	76.89693
	363	110.3223039		363	109.5091
0.5	318	28.73984523	1	318	28.38
	333	49.90865314		333	49.38714
	348	77.23502482		348	76.5442
	363	109.9250516		363	109.0748

In tables (14) and (15) similar patterns for other concentrations can be seen as well.

iv. Effect of flow rate on feed side:

The increase in flow rate on feed side was accompanied by an increase in permeate generation. For instance, when flow rate was increased from 50 L/hr to 100 L/hr for concentration of 1 M and Tb of 318 K, the permeate increased from 20.50 L/m^2.hr to 28.38L/m^2.hr

This increase in flux can be explained by the fact that at a higher Reynolds number **(17,300 for v=2.2 m/s as compared to 6100 for v=1.1 m/s)** the turbulence increases which improves heat, mass transfer from water solution (feed) to the surface of hydrophobic membrane, resulting in an increased flux rate.

v. Temperature Polarization Coefficient (TPC)

For the purpose of this study, owing to the presence of vacuum on permeate side, the boundary layer on the permeate side was not relevant and therefore the definition given by (11) was used to compute TPC [56]. Figures (18) and (19) show the TPC values for different concentration and Tb values.

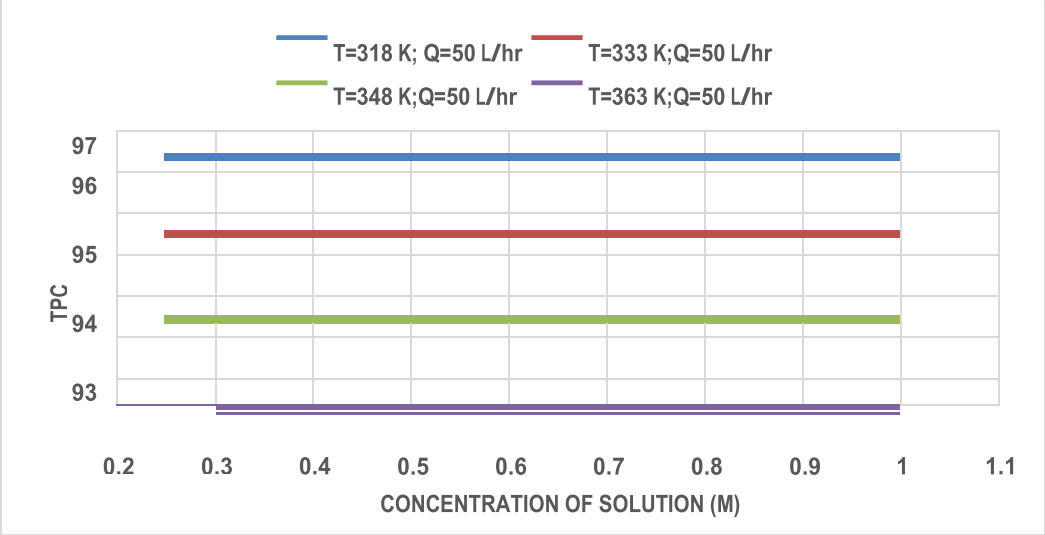

Figure 22- TPC as a function of solution concentration for different values of temperature for feed flow rate of 50 L/hr

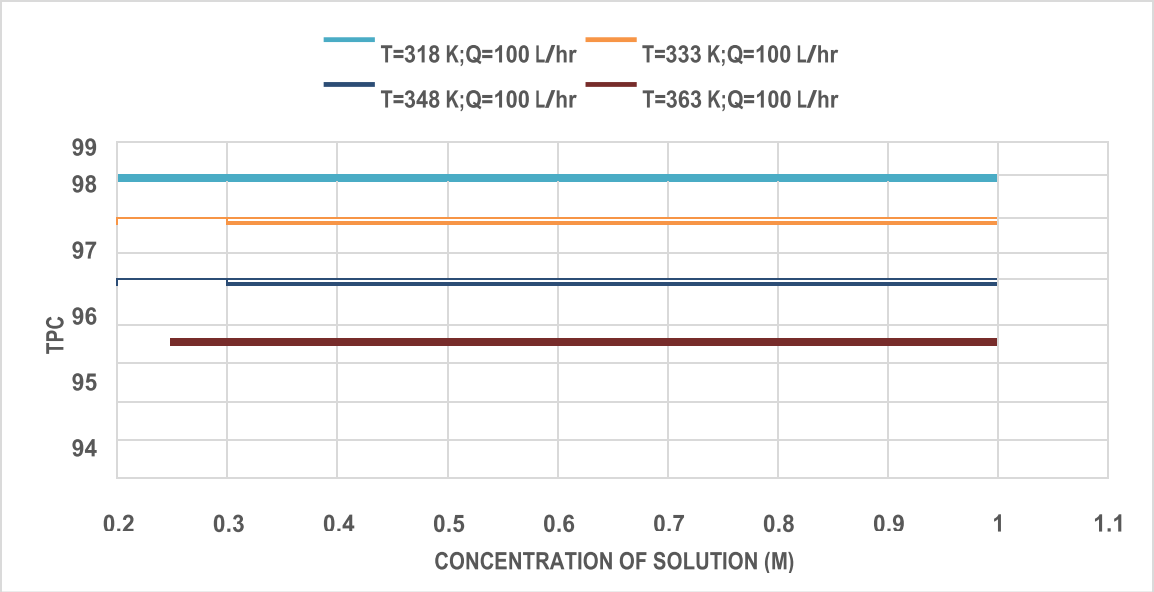

Figure 23- TPC as a function of solution concentration for different values of temperature for feed flow rate of 100 L/hr

The TPC increases when the feed velocity is increased. This means that the increase in turbulence enhances the heat transfer and the difference between the temperatures of the bulk feed solution and the solution at the membrane interface decreases. For Tb of 318 K and 1 M solution, the TPC increases from 96.4 to 98.1 indicating a decrease in polarization effect when feed flow rate is increased from 50 L/hr to 100 L/hr.

The increase in concentration of solution decreased the polarization effect as indicated by a positive slope for the graphs. This is because the increased salt concentration decreases the pressure of water vapours, thereby decreasing the vapor flux (as discussed before). Decrease in vapour pressure means decrease in separation and thus less heat is being taken away in the form of latent heat by water vapors. This ultimately decreases the difference in temperature between the bulk feed solution and the membrane interface. For Tb of 333 K and Q of 50 L/hr, the TPC value increased from 94.46 to 94.52 when concentration was increased from 0.25 M to 1.0 M.

Table 20- Change in TPC with Tb for various concentration (flow rate of 50 L/hr)

T_b (K)	Molarity	TPC	T_b (K)	Molarity	TPC
318	0.25	96.33553953	348	0.25	92.40612
	0.5	96.35257597		0.5	92.4303
	0.75	96.37039969		0.75	92.45564
	1	96.38898997		1	92.4821
333	0.25	94.45798982	363	0.25	90.26982
	0.5	94.4790261		0.5	90.29639
	0.75	94.50105246		0.75	90.32423
	1	94.52404583		1	90.35333

Table 21- Change in TPC with Tb for various concentration (flow rate of 100 L/hr)

T_b (K)	Molarity	TPC	T_b (K)	Molarity	TPC
318	0.25	98.0646217	348	0.25	95.25482
	0.5	98.07574657		0.5	95.27458
	0.75	98.08736635		0.75	95.29527
	1	98.08736635		1	95.31685
333	0.25	96.79331324	363	0.25	93.52915
	0.5	96.80892817		0.5	93.55245
	0.75	96.82525477		0.75	93.57684
	1	96.84227264		1	93.60232

CHAPTER 5: CONCLUSION AND RECOMMENDATION

Based on the results of mathematical modeling and computational analysis, the application of VMD seems a promising solution for the treatment of industrial wastewater. However, there still exists the need to perform a financial analysis to determine the commercial feasibility of the solution against conventional chemical and pressure drive filtration processes currently being employed in industry to treat wastewater.

The results obtained from mathematical modelling shows trend that are congruent with existing body of knowledge on VMD. Increase in temperature and feed velocity have a positive impact on the permeate flux while increase in feed solution concentration has a negative effect.

The next step in mathematical modelling can be optimization analysis during which the optimal conditions are determined for a particular value of permeate flux. Moreover, this mathematical modeling was performed assuming a 2D geometry and average pore size. A better model can be obtained by considering the pore size distribution. However, this will increase the complexity of the model several fold.

As pointed out earlier many industrialists in developing countries take advantage of poor governance and regulation issues to get away with discharge of untreated wastewater into river bodies used to supply water to human population. By developing an affordable solution, the industrialists can be encouraged to adopt wastewater treatment. In this regard, solar energy and waste heat can be used to drive the VMD process. This will decrease the cost associated

with the process. Therefore a future step could be the investigation of the benefit obtained by using a renewable energy source or waste heat.

Apart from its complexity, the reason why MD and VMD in particular is not completely commercialized is its operating cost. To counter this, VMD can be integrated with other cheaper filtration techniques like reverse osmosis to reduce the running cost.

REFRENCES

[1] UNESCO. The United Nations World Water Development Report 2017.Retrieved from: http://unesdoc.unesco.org/images/0024/002471/247153e.pdf

[2] F.W. Ntengwe. *An overview of industrial wastewater treatment and analysis as means of preventing pollution of surface and underground water bodies—the case of Nkana Mine in Zambia.* Physics and Chemistry of the Earth, (2005). 30 726–734

[3] M. Gryta, K. Karakulski, A.W. Morawski, *Purification of oily wastewater by hybrid UF/MD*, Water Res. 35 (15) (2001) 3665–3669.

[4] A. Criscuoli, E. Drioli, *Energetic and exergetic analysis of an integrated membrane desalination system*, Desalination 124 (1–3) (1999) 243–249.

[5] H. Kurokawa, T. Sawa, *Heat recovery characteristics of membrane distillation, Heat transfer*-Japanese Research 25 (1996) 135–150.

[6] J. Blanco Gálvez, L. García-Rodríguez, I. Martín-Mateos, *Seawater desalination by an innovative solar-powered membrane distillation system: the MEDESOL project,* Desalination 246 (1–3) (2009) 567–576.

[7] P.P. Zolotarev, et al., *Treatment of waste water for removing heavy metals by membrane distillation*, J. Hazard. Mater. 37 (1) (1994) 77–82.

[8] J. Walton, et al., *Solar and waste heat desalination by membrane distillation*, College of Engineering University of Texas, El Paso, 2004.

[9] Abdullah Alkhudhiri , Naif Darwish ,and Nidal Hilal. *Membrane distillation: A comprehensive review.*Desalination, 2012. 287 p 2–18

[10] Mostafa Abd El-Rady Abu-Zeid a,b, Yaqin Zhang a, Hang Donga, Lin Zhang a,□, Huan-Lin Chen a, Lian Houa, *A comprehensive review of vacuum membrane distillation technique* Desalination 356 (2015) 1–14

[11] F. Laganà, G. Barbieri, E. Drioli, *Direct contact membrane distillation: modelling and concentration experiments*, J. Membr. Sci. 166 (1) (2000) 1–11.

[12] J. Walton, et al., *Solar and waste heat desalination by membrane distillation*, College of Engineering University of Texas, El Paso, 2004.

[13] M.C. García-Payo, M.A. Izquierdo-Gil, C. Fernández-Pineda, *Air gap membrane distillation of aqueous alcohol solutions*, J. Membr. Sci. 169 (1) (2000) 61–80.

[14] S. Kimura, S.-I. Nakao, S.-I. Shimatani, *Transport phenomena in membrane distillation*, J. Membr. Sci. 33 (3) (1987) 285–298.

[15] F.A. Banat, J. Simandl, *Membrane distillation for dilute ethanol: separation from aqueous streams*, J. Membr. Sci. 163 (2) (1999) 333–348.

[16] Mohamed Khayet, *Membranes and theoretical modeling of membrane distillation: A review*. Advances in Colloid and Interface Science, 2011. 164 p 56-88

[17] M.C. García-Payo, et al., *Separation of binary mixtures by thermostatic sweeping gas membrane distillation: II. Experimental results with aqueous formic acid solutions*, J. Membr. Sci. 198 (2) (2002) 197–210.

[18] M.S. El-Bourawi, et al., *A framework for better understanding membrane distillation separation process*, J. Membr. Sci. 285 (1–2) (2006) 4–29.

[19] Kevin W. Lawson and Douglas R. Lloyd. *Membrane distillation*. Journal of Membrane Science,1997. 124 p 1-25

[20] D.E. Suk, T. Matsuura, H.B. Park, Y.M. Lee, *Development of novel surface modified phase inversion membranes having hydrophobic surface-modifying macromolecule (nSMM) for vacuum membrane distillations*, Desalination 261 (3) (2010) 300–312.

[21] A.M. Urtiaga, G. Ruiz, I. Ortiz, *Kinetic analysis of the vacuummembrane distillation of the chloroform form aqueous solutions*, J. Membr. Sci. 165 (2000) 99–110.

[22] N. Couffin, C. Caufin, C. Cabassud, V. Lahoussine-Turcaud, *A new process to remove halogenated VOCs or drinking water production: vacuum membrane distillation*,

Desalination 117 (1–3) (1998) 233–245.

[23] M.C. Garcia-Payo, M.A. Izquierdo-Gil, C. Fernandez-Pineda, *Air gap membrane distillation of aqueous alcohol solutions*, J. Membr. Sci. 169 (2000) 61–80.

[24] M.S. EL-Bourawi, M. Khayet, R. Ma, Z. Ding, Z. Li, X. Zhang, *Application of vacuum membrane distillation for ammonia removal*, J. Membr. Sci. 301 (2007) 200–209

[25] B. Wu, X. Tan, K. Li, W.K. Teo, *Preparation and characterization of poly(vinylidene fluoride) hollow fiber membranes for vacuum membrane distillation*, J. Appl. Polym. Sci. 106 (2007) 1482–1495.

[26] J. Chen, Y. Zhang, Y. Wang, X. Ji, L. Zhang, X. Mi, H. Huang, *Removal of inhibitors from lignocellulosic hydrolyzates by vacuum membrane distillation*, Bioresour. Technol. 144 (2013) 680–683.

[27] E. Hoffman, D. Pfenning, E. Philippsen, P. Schwahn, M. Seiber, D.Woermann, *Evaporation of alcohol/water mixtures through hydrophobic porous membranes*, J. Membr. Sci. 34 (2) (1987) 199–206.

[28] S. AL-Asheh, F. Banat, M. Qtaishat, M. AL-Khateeb, *Concentration of sucrose solutions via vacuum membrane distillation*, Desalination 195 (2006) 60–68.

[29] Y. Yun, R. Ma,W. Zhang, A.G. Fane, J. Li, *Direct contact membrane distillation*

mechanism for high concentration NaCl solutions, Desalination 188 (1–3) (2006) 251–262.

[30] N. Diban, O.C. Voinea, A. Urtiaga, I. Ortiz, *Vacuum membrane distillation of the main pear aroma compound: experimental study and mass transfer modeling*, J. Membr. Sci. 326 (2009) 64–75.

[31] S. Bandini, G.C. Sarti, *Concentration of must through vacuum membrane distillation*, Desalination 149 (2002) 253–259.

[32] Z. Zhao, F. Ma, W. Liu, D. Liu, *Concentration of ginseng extracts aqueous solutions by vacuum membrane distillation. 2. Theory analysis of critical operating conditions and experimental confirmation*, Desalination 267 (2011) 147–153.

[33] T. Mohammadi, M. Akbarabadi, *Separation of ethylene glycol solution by vacuum membrane distillation (VMD)*, Desalination 181 (1–3) (2005) 35–41.

[34] J.P. Mericq, S. Laborie, C. Cabassud, *Vacuum membrane distillation of seawater reverse osmosis brines*, Water Resour. 44 (18) (2010) 5260–5273.

[35] M. Gryta, M. Tomaszewska, K. Karakulski, *Wastewater treatment by membrane distillation*, Desalination 198 (2006) 67–73.

[36] M. Sivakumar, M. Ramezanianpour, G.O. Halloran, *Mine water treatment using a vacuum membrane distillation system*, ICESD 2013: January 19–20, Dubai, UAE, APCBEE Procedia, 5, 2013, pp. 157–162.

[37] G. Zakrzewska-Trznadel, M. Harasimowicz, A.G. Chmielewski, *Concentration of radioactive components in liquid low-level radioactive waste by membrane distillation*, J. Membr. Sci. 163 (2) (1999) 257–264.

[38] A. Criscuoli, J. Zhong, A. Figoli, M.C. Carnevale, R. Huang, E. Drioli, *Treatment of the dye solutions by vacuum membrane distillation*, Water Resour. 42 (2008) 5031–5037

[39] F. Macedonio, E. Drioli, *Pressure-driven membrane operations and membrane distillation technology integration for water purification*, Desalination 223 (2008) 396 409.

[40] A. Criscuoli, P. Bafaro, E. Drioli, *Vacuum membrane distillation for purifying waters containing arsenic*, Desalination 323 (2013) 17–21.

[41] N. Tang, H. Zhang, W. Wang, *Computational fluid dynamics numerical simulation of vacuum membrane distillation for aqueous NaCl solution*, Desalination 274 (2011) 120–129.

[42] F.A. Banat, J. Simandl, *Membrane distillation for dilute ethanol: separation from aqueous streams*, J. Membr. Sci. 163 (2) (1999) 333–348.

[43] M.A. Izquierdo-Gil, G. Jonsson, *Factors affecting flux and ethanol separation*

performance in vacuum membrane distillation (VMD), J. Membr. Sci. 214 (1) (2003) 113–130.

[44] Z. Wang, Z. Gu, S. Feng, Y. Li, *Application of vacuum membrane distillation to lithium bromide absorption refrigeration system*, Int. J. Refrig. 32 (2009) 1587–1596.

[45] Heiyan Zhang, Meiqin Liu, De Sun*, Bingbing Li, Pengxian Li .*Evaluation of commercial PTFE membranes for desalination of brine water through vacuum membrane distillation* Chemical Engineering and Processing 110 (2016) 52–63

[46] Gayathri Naidu, Yongjun Choi, Sanghyun Jeong ,Tae Mun Hwang ,and Saravanamuthu Vigneswaran. *Experiments and modeling of a vacuum membrane distillation for high saline water*. Journal of Industrial and Engineering Chemistry, 2014. 20 p. 2174–2183

[47] L. Zhang, Y.Wang, L.H. Cheng, X. Xu,H. Chen, *Concentration of lignocellulosic hydrolyzates by solar membrane distillation*, Bioresour. Technol. 123 (2012) 382–385.

[48] Rosalam Sarbatly, Chel-Ken Chiam .*Evaluation of geothermal energy in desalination by vacuum membrane distillation*. Applied Energy 112 (2013) 737–746

[49] Z. Wang, Z. Gu, S. Feng, Y. Li, *Application of vacuum membrane distillation to lithium bromide absorption refrigeration system*, Int. J. Refrig. 32 (2009) 1587–1596.

[50] J.I. Mengual, M. Khayet , and M.P. Godino. *Heat and mass transfer in vacuum*

membrane distillation. International Journal of Heat and Mass Transfer, 2004. 47 p 865–875

[51] S. Bandini, C. Gostoli, and G.C. Sarti. *Separation efficiency in vacuum membrane distillation*. Journal of Membrane Sciences, 1992. 73 p 217–229.

[52] Ahmad S. Alsaadi, Lijo Francis, Gary L. Amy, and Noreddine Ghaffour, *Experimental and theoretical analyses of temperature polarization effect in vacuum membrane distillation.* Journal of Membrane Science, 2014. 471 p 138-148

[53] Heiyan Zhang, Meiqin Liu, De Sun, Bingbing Li, and Pengxian Li. *Evaluation of commercial PTFE membranes for desalination of brine water through vacuum membrane distillation.* Chemical Engineering and Processing: Process Intensification,2016. 110 p 52-63

[54] R.W. Schofield, A.G. Fane, and C.J.D. Fell. *Heat and mass-transfer in membrane distillation*, Journal of Membrane Sciences,1987. 33 p 299–313.

[55] J.P. Mericq, S. Laborie, and C. Cabassud. *Evaluation of systems coupling vacuum membrane distillation and solar energy for sea water desalination*. Chemical Engineering Journal, 2011. 166 p 596–606.

[56] F. Banat, S. Al-Asheh, and M. Qtaishat. *Treatment of waters colored with methylene blue dye by vacuum membrane distillation*. Desalination, 2005. 174 p 87–96.

[57] S. Bandini, C. Gostoli, and G.C. Sarti. *Separation efficiency in vacuum membrane*

distillation. Journal of Membrane Sciences, 1992. 73 p 217–229.

[58] S.G. Lovineh, M. Asghari, and B. Rajaei. *Numerical simulation and theoretical study on simultaneous effects of operating parameters in vacuum membrane distillation*. Desalination, 2013. 314 p 59–66.

[59] M. Khayet and T. Matsuura. *Pervaporation and vacuum membrane distillation processes: modeling and experiments*. AIChEJ, 2004. 50 p 1697–1712.

[60] Na Tang, Huanju Zhang, Wei Wang, *Computational fluid dynamics numerical simulation of vacuum membrane distillation for aqueous NaCl solution*, Desalination 274 (2011) 120-129.

[61] I. F. Macdonald, M. S. El-Sayed, K. Mow, F. A. L. Dullien, *Flow through Porous Media-the Ergun Equation Revisited*, Ind. Eng. Chem. Fundamen., 1979, 18 (3), pp 199–208

[62] Kiyotaka Sakai, Takeshi Koyano and Toshihito Muroi, *Effects of Temperature and Concentration Polarization on Water Vapour Permeability for Blood in Membrane Distillation*, The Chemical Engineering Journal, 38 (1988) B33 - B39

APPENDIX I: MATLAB CODE

The code used in MATLAB is shown below for a particular set of operating conditions.

```
%National University of Sciences & Technology

%FYP Mathematical Modeling: Heat & Mass Transfer in VMD

%5th February

clc;

clear;

%All units in SI

%Feed Temperature (Tf)

T_f = 310;

%Feed concentration (Cf)

C_f = 1;

%Kinematic viscosity of water

nu = 0.801*10^-6;

%------------------------------------------------------------------------%

%d_h is hydraulic diameter

%D is diffusion coefficient of solute

%Re is Reynold's number

%rho is density of water,V is free stream velocity,L is length of surface

%Q is flow rate,V is flow velocity,
```

```
%A=t_channel*length_channel ;

%d_h = (4*A)/((2*length_channel)+(2*t_channel));

d_h=0.77*10^-2;
Q=50/(3600*1000);
Area=3.1415*((d_h/2)^2);
V=Q/Area;
%Calculation of Re

D= 3.96*10^-9;

%diffusion coeff for salt

rho = 1000;

Sc=0;

Re=(d_h*V)/nu;

%Ref for nu:https://www.engineeringtoolbox.com/water-dynamic-kinematic-viscosity-d_596.html

%mew is dynamics viscosity and D is mass diffusivity

%Calculate heat transfer coefficient h_w

%T_f and T_m are temp of bulk and interfacial region

%Hv is latent heat of vaporization,k_m is thermal conductivity of water

h_w = 0;
T_m= 0 ;

Hv = 2414.2*10^3 ;%in J/kg.Cengel

k_m=0.6262; %Ref.Cengel.For liq water

Pr = 4.626;%Ref.Cengel.For liq water

L=18*10^-2;    %lenth of channel
```

```
%equations

%calculation of  Nusselt number
If Re< 2000

Nu = 1.86 *( (Re*Pr*d_h) / L )^0.33;

end

if 4000>Re && Re>2100

Nu=0.116*((Re^0.67)-125)*(Pr^1/3)*(1+(d_h/L)^2/3);

end

if Re > 4000

Nu = 0.023*(Re^0.8)*(Pr^0.33);

end.

%calculation of heat transfer coefficient

h_w = (k_m*Nu) / d_h;



%-------------------------------------------------------------------------%

%Mole fraction of salt is calculated (chromium sulphate)

moles_salt=C_f;
moles_water=392.16;

moles_total= moles_water + moles_salt;
molefraction_salt=moles_salt/moles_total;

%-------------------------------------------------------------------------%
```

```
    %Calcualtion on net MD coefficent (B)
%porosity
Omega = 0.75;
%membrane thickness
Delta = 165*10^-6;
%tortuoisty
tau = 2;
%pore size
r=0.2*10^-6
%M is molar mass of water,R is general gas constant
M=18;
R= 8314.472;
T=T_f;


B=1.064*((r*omega)/(delta*tau))*((M/(R*T))^(1/2));
B_per_hr=B*3600;
    %The values calculated above are used in Maple to solve system equations
    %and obtain flux J and temperature at membrane
```

APPENDIX II: MAPLE CODE

The code used in MAPLE is shown below for a particular set of operating conditions.

$Tb := 310.2;$

$B := \frac{0.00165}{3600};$

$Pvac := 4500;$

$Pv := 450;$

$h := 7.619121759849392 \cdot 10^{3};$

$gv := 2414.2 \cdot 10^{3};$

$x\_salt := 0.017680339462518;$

310.2

$4.583333333\,10^{-7}$

$f3 := Ti \rightarrow (1$

4500

450

$2.4142000\,10^{6}$

7619.121760

0.017680339462518

$$f3 := Ti \rightarrow (1 - x\_salt) \cdot \left(1 - 0.5 \cdot x\_salt - 10 \cdot x\_salt^{2}\right) \cdot e^{\left(23.1964 - \frac{3816.44}{Ti - 46.13}\right)};$$

$$Ti \rightarrow (1 - x\_salt)\left(1 + (-1) \cdot 0.5\, x\_salt - 10\, x\_salt^{2}\right) e^{23.1964 + \frac{(-1) \cdot 3816.44}{Ti - 46.13}}$$

$$Ti \quad Tb - \left(\frac{Tb - Ti}{J}\right) \cdot B \cdot (f3(Ti) - Pv);$$

$$Ti = 310.2 - \frac{4.583333333\,10^{-7}\,(310.2 - Ti)\left(0.9705651118\, e^{23.1964 - \frac{3816.44}{Ti - 46.13}} - 450\right)}{J}$$

$$J = \frac{h \cdot (Tb - Ti)}{gv};$$

$$J = 0.9789791940 \quad 0.003155961296\, Ti$$

$$sys := \left\{ Ti = Tb - \left(\frac{Tb - Ti}{J} \right) \cdot B \cdot (f3(Ti) - Pv),\ J = \frac{h \cdot (Tb - Ti)}{gv} \right\};$$

$$\left| J = 0.9789791940 \quad 0.003155961296\, Ti,\ Ti = 310.2 \right.$$

$$\left. - \frac{4.583333333\, 10^{-7}\, (310.2 - Ti) \left(0.9705651118\, e^{23.1964 \quad \frac{3816.44}{Ti - 46.13}} - 450 \right)}{J} \right|$$

$$solve(\ sys,\ \{Ti, J\}\ );$$

$$\{J = -1.920000000\, 10^{-11},\ Ti = 310.2000000\},\ \{J = 0.002467065568,\ Ti = 309.4182840\}$$

APPENDIX III: ARDUINO CODE FOR FEED SIDE

```
// This code helps measure and display the reservoir temperature, flow rate
// and controls heating coil through relay

// temp sensor library
#include <OneWire.h>
// relay
#define relay A8
// lcd library
#include <LiquidCrystal.h>


byte statusLed    = 13;
byte sensorInterrupt = 0; // 0 = digital pin 4
byte sensorPin       = 2;

// The hall-effect flow sensor outputs approximately 4.5 pulses per second per
// litre/minute of flow.
float calibrationFactor = 4.5;

volatile byte pulseCount;

float flowRate;
unsigned int flowMilliLitres;
unsigned long totalMilliLitres;
```

```
unsigned long oldTime;
const int rs = 13, en = 12, d4 = 8, d5 = 7, d6 = 6, d7 = 5;
LiquidCrystal lcd(rs, en, d4, d5, d6, d7);
OneWire ds(4); // on pin 3 (a 4.7K resistor is necessary)


void setup(void) {
  Serial.begin(9600);
  // Initialize a serial connection for reporting values to the host
  Serial.begin(9600);

  // Set up the status LED line as an output
  pinMode(statusLed, OUTPUT);
  digitalWrite(statusLed, HIGH); // We have an active-low LED attached

  pinMode(sensorPin, INPUT);
  digitalWrite(sensorPin, HIGH);

  pulseCount        = 0;
  flowRate          = 0.0;
  flowMilliLitres   = 0;
  totalMilliLitres = 0;
  oldTime           = 0;

  // The Hall-effect sensor is connected to pin 2 which uses interrupt 0.
  // Configured to trigger on a FALLING state change (transition from HIGH
  // state to LOW state)
  attachInterrupt(sensorInterrupt, pulseCounter, FALLING);
```

```
  //relay var definition
  pinMode(relay, OUTPUT);

   // set up the LCD's number of columns and rows:
  lcd.begin(16,2);
  // Print a message to the LCD.
  lcd.print("T_res");
}


void loop(void) {
  byte i;
  byte present = 0;
  byte type_s;
  byte data[12];
  byte addr[8];
  float celsius, fahrenheit;
if((millis() - oldTime) > 1000)    // Only process counters once per second
  {
    // Disable the interrupt while calculating flow rate and sending the value to
    // the host
    detachInterrupt(sensorInterrupt);

    // Because this loop may not complete in exactly 1 second intervals we calculate
    // the number of milliseconds that have passed since the last execution and use
    // that to scale the output. We also apply the calibrationFactor to scale the output
    // based on the number of pulses per second per units of measure (litres/minute in
    // this case) coming from the sensor.
    flowRate = ((1000.0 / (millis() - oldTime)) * pulseCount) / calibrationFactor;
```

```
  // Note the time this processing pass was executed. Note that because we've
  // disabled interrupts the millis() function won't actually be incrementing right
  // at this point, but it will still return the value it was set to just before
  // interrupts went away.
  oldTime = millis();

  // Divide the flow rate in litres/minute by 60 to determine how many litres have
  // passed through the sensor in this 1 second interval, then multiply by 1000 to
  // convert to millilitres.
  flowMilliLitres = (flowRate / 60) * 1000;

  // Add the millilitres passed in this second to the cumulative total
  totalMilliLitres += flowMilliLitres;

  unsigned int frac;

  // Print the flow rate for this second in litres / minute
  Serial.print("Flow rate: ");
  Serial.print(int(flowRate)); // Print the integer part of the variable
  Serial.print("L/min");
  Serial.print("\t");       // Print tab space

  // Print the cumulative total of litres flowed since starting
  Serial.print("Output Liquid Quantity: ");
  Serial.print(totalMilliLitres);
  Serial.println("mL");
Serial.print("\t");       // Print tab space
Serial.print(totalMilliLitres/1000);
```

```
Serial.print("L");


  // Reset the pulse counter so we can start incrementing again
  pulseCount = 0;

  // Enable the interrupt again now that we've finished sending output
  attachInterrupt(sensorInterrupt, pulseCounter, FALLING);
}
if ( !ds.search(addr)) {
  //Serial.println("No more addresses.");
  Serial.println();
  ds.reset_search();
  delay(250);
  return;
}


//Serial.print("ROM =");
for( i = 0; i < 8; i++) {
Serial.write(' ');
 // Serial.print(addr[i], HEX);
}

if (OneWire::crc8(addr, 7) != addr[7]) {
    Serial.println("CRC is not valid!");
    return;
}
Serial.println();
```

```
  // the first ROM byte indicates which chip
  switch (addr[0]) {
    case 0x10:
      Serial.println(" Chip = DS18S20"); // or old DS1820
      type_s = 1;
      break;
    case 0x28:
      Serial.println(" Chip = DS18B20");
      type_s = 0;
      break;
    case 0x22:
      Serial.println(" Chip = DS1822");
      type_s = 0;
      break;
    default:
      Serial.println("Device is not a DS18x20 family device.");
      return;
  }

  ds.reset();
  ds.select(addr);
  ds.write(0x44);        // start conversion, use ds.write(0x44,1) with parasite power on at
the end

  delay(1000);     // maybe 750ms is enough, maybe not
  // we might do a ds.depower() here, but the reset will take care of it.

  present = ds.reset();
```

```
 ds.select(addr);
 ds.write(0xBE);         // Read Scratchpad

// Serial.print(" Data = ");
 //Serial.print(present, HEX);
// Serial.print(" ");
 for ( i = 0; i < 9; i++) {           // we need 9 bytes
   data[i] = ds.read();
   //Serial.print(data[i], HEX);
  // Serial.print(" ");
 }
 //Serial.print(" CRC=");
// Serial.print(OneWire::crc8(data, 8), HEX);
 //Serial.println();

 // Convert the data to actual temperature
 // because the result is a 16 bit signed integer, it should
 // be stored to an "int16_t" type, which is always 16 bits
 // even when compiled on a 32 bit processor.
 int16_t raw = (data[1] << 8) | data[0];
 if (type_s) {
   raw = raw << 3; // 9 bit resolution default
   if (data[7] == 0x10) {
     // "count remain" gives full 12 bit resolution
     raw = (raw & 0xFFF0) + 12 - data[6];
   }
 } else {
   byte cfg = (data[4] & 0x60);
   // at lower res, the low bits are undefined, so let's zero them
```

```
    if (cfg == 0x00) raw = raw & ~7; // 9 bit resolution, 93.75 ms
    else if (cfg == 0x20) raw = raw & ~3; // 10 bit res, 187.5 ms
    else if (cfg == 0x40) raw = raw & ~1; // 11 bit res, 375 ms
    //// default is 12 bit resolution, 750 ms conversion time
   }
   celsius = (float)raw / 16.0;
   fahrenheit = celsius * 1.8 + 32.0;
   Serial.print(" Temperature = ");
   Serial.print(celsius);
   Serial.print(" Celsius, ");
   Serial.print(fahrenheit);
   Serial.println(" Fahrenheit");
   Serial.print("\t");

//This part cotrols relay
   if (celsius<75)
  {digitalWrite(relay, LOW);

  }
  if (celsius>75)
  {digitalWrite(relay,HIGH);

}
  // set the cursor to column 0, line 1
   // (note: line 1 is the second row, since counting begins with 0):

   lcd.setCursor(0, 1);
   // prints what you want
   //write celsius for temperature,flowRate for L/min flow rate of water
```

```
  lcd.print(celsius);
}
void pulseCounter()
{
  // Increment the pulse counter
  pulseCount++;
}
```

APPENDIX V: ARDUINO CODE FOR SALINITY MEASUREMENT

```
 #include <OneWire.h>
#include <DallasTemperature.h>
//**************** User Defined Variables*************************//
 //-----------  Do not Replace R1 with a resistor lower than 300 ohms     ----------
//#########################################################################

int R1= 1000;
int Ra=25; //Resistance of powering Pins
int ECPin= A0;
int ECGround=A1;
int ECPower =A4;


//*********** Converting to ppm [Learn to use EC it is much better**************//
// Hana      [USA]       PPMconverion:  0.5
// Eutech    [EU]        PPMconversion:  0.64
//Tranchen [Australia] PPMconversion: 0.7
float PPMconversion=0.7;

//*************Compensating for temperature*********************************//
```

```
//The value below will change depending on what chemical solution we are measuring
//0.019 is generaly considered the standard for plant nutrients [google "Temperature compensation EC" for more info float TemperatureCoef = 0.019; //this changes depending on what chemical we are measuring
//************ Cell Constant For Ec Measurements*************//
//Mine was around 2.9 with plugs being a standard size they should all be around the same
//But If you get bad readings you can use the calibration script and fluid to get a better estimate for K
float K=2.88;

//************ Temp Probe Related ************************//
#define ONE_WIRE_BUS 4          // Data wire For Temp Probe is plugged into pin 3 on the Arduino

//****************************** END Of Recomended User Inputs *****************************************************************//


OneWire oneWire(ONE_WIRE_BUS);// Setup a oneWire instance to communicate with any OneWire devices
DallasTemperature sensors(&oneWire);// Pass our oneWire reference to Dallas Temperature.
```

```
float Temperature=10;
float EC=0;
float EC25 =0;
int ppm =0;
float raw= 0;
float Vin= 5;
float Vdrop= 0;
float Rc= 0;
float buffer=0;

//*****************Setup - runs Once and sets pins etc***********************//
void setup()
{
  Serial.begin(9600);
  pinMode(ECPin,INPUT);
  pinMode(ECPower,OUTPUT);//Setting pin for sourcing current
  pinMode(ECGround,OUTPUT);//setting pin for sinking current
  digitalWrite(ECGround,LOW);//We can leave the ground connected permanantly

  delay(100);// gives sensor time to settle
  sensors.begin();
  delay(100);
  //** Adding Digital Pin Resistance to [25 ohm] to the static Resistor *********//
```

```
  // Consule Read-Me for Why, or just accept it as true
  R1=(R1+Ra);// Taking into acount Powering Pin Resitance

  Serial.println("ElCheapo Arduino EC-PPM measurments");
  Serial.println("By: Michael Ratcliffe Mike@MichaelRatcliffe.com");
  Serial.println("Free software: you can redistribute it and/or modify it under GNU ");
  Serial.println("");
  Serial.println("Make sure Probe and Temp Sensor are in Solution and solution is well mixed");
  Serial.println("");
  Serial.println("Measurments at 5's Second intervals [Dont read Ec morre than once every 5 seconds]:");


};
//******************** End of Setup ******************************//

//******************** Main Loop - Runs Forever *************************//
//Moved Heavy Work To subroutines so you can call them from main loop without cluttering the main loop
```

```
void loop()
{

GetEC();          //Calls Code to Go into GetEC() Loop [Below Main Loop] dont call this more that 1/5 hhz [once every five seconds] or you will polarise the water
PrintReadings(); // Cals Print routine [below main loop]

delay(5000);

}
//************************************** End Of Main Loop**************//

//************ This Loop Is called From Main Loop************************//
void GetEC(){

//**********Reading Temperature Of Solution ******************//
sensors.requestTemperatures();// Send the command to get temperatures
Temperature=sensors.getTempCByIndex(0); //Stores Value in Variable


//************Estimates Resistance of Liquid ****************//
digitalWrite(ECPower,HIGH);
```

```
raw= analogRead(ECPin);
raw= analogRead(ECPin);// This is not a mistake, First reading will be low beause if charged a capacitor
digitalWrite(ECPower,LOW);

//****************** Converts to EC **************************//
Vdrop= (Vin*raw)/1024.0;
Rc=(Vdrop*R1)/(Vin-Vdrop);
Rc=Rc-Ra; //acounting for Digital Pin Resitance
EC = 1000/(Rc*K);
//*************Compensating For Temperaure********************//
EC25 = EC/ (1+ TemperatureCoef*(Temperature-25.0));
ppm=(EC25)*(PPMconversion*1000);
;}
//*************************** End OF EC Function ***************************//
//***This Loop Is called From Main Loop- Prints to serial usefull info ***//
void PrintReadings(){
Serial.print("Rc: ");
Serial.print(Rc);
Serial.print(" EC: ");
Serial.print(EC25);
Serial.print(" Simens  ");
```

```
Serial.print(p
pm);
Serial.print("
ppm ");
Serial.print(T
emperature);
Serial.println(
" *C ");

/*
//********** Usued for Debugging
************ Serial.print("Vdrop: ");
Serial.println(
Vdrop);
Serial.print("
Rc: ");
Serial.println(
Rc);
Serial.print(E
C);
Serial.println(
"Siemens");
//********** end of Debugging Prints **********
*/
```

```
};
```